Formulation, Optimization & Evaluation of Nanoemulgel Loaded with Roxithromycin and Eugenol for Effective Periodontitis Management

Rishabh Maurya[1]*, Ashu Mittal[2], Gaurav Tiwari[3]

*[*1]Research Scholar, Teerthanker Mahaveer College of Pharmacy, Teerthanker Mahaveer University, Moradabad- Delhi Road, 244001. India*

[2]Professor and Principal, Teerthanker Mahaveer College of Pharmacy, Teerthanker Mahaveer University, Moradabad-Delhi Road, 244001. India

[3]Professor, PSIT-Pranveer Singh Institute of Technology (Pharmacy), Kalpi Road, Bhauti, Kanpur-209305. India

**Author for correspondence:*

Mr. Rishabh Maurya
Research Scholar
Teerthanker Mahaveer College of Pharmacy (TMCOP),
Teerthanker Mahaveer University (TMU),
Delhi Road, Moradabad, Uttar Pradesh (244001), India
Email: mirishabh14@gmail.com

ABSTRACT

A new RXN nanoemulgel based on carbopol 934 was created to be used in intra-pocket periodontal therapy that has to provide better retention and the delivery of the drug to the target area. Spontaneous emulsification generated RXN nanoemulsions with the excipients: oil phase (eugenol), surfactant (Tween 80), co-surfactant (PEG 400), aqueous phase (water). A Box–Behnken experimental design (3-factor, 3-level) was utilized to optimize the formulation in which the concentration (v/v) of oil (X_1), S_{mix} surfactant and co-surfactant (X_2), and water (X_3) were the independent variables. The dependent variables were to be optimized by globule size (Y_1), heterogeneity index /polydispersity index (PDI) (Y_2), and zeta potential (Y_3). Globe size, PDI, zeta potential, viscosity and morphology of surface of the nanoemulsions were characterised and the developed nanoemulgel was also tested with content of drug, pH, mucoadhesion strength, on syringeability, temperature of sol-gel transition, viscosity and release of drug. The optimized formulation was 13% (oil), 37% (S_{mix}) and 50 % (water) and that provided a globule size 118.3 ± 7 nm, PDI 0.387 ± 0.023 and zeta potential -21.73 ± 5.67 mV. The analysis of surface morphology and globule size done by transmission electron microscopy (TEM) disclosed the optimized nanoemulgel had mainly uniform and spherical particles diameter (22.10 to 180.10 nm). The optimized RXN nanoemulgel was found to have good syringeability and an appropriate viscosity, and sol-gel transition, which makes it easy to apply intra-pocket. It demonstrated a sustained release of the drug in *ex-vivo* and a high antibacterial effect of *S. aureus* (24.1 ± 0.34 mm) and *E. coli* (18.7 ± 0.36 mm). These findings affirm its ability as a useful localized drug delivery in periodontal therapy.

Keywords: Periodontitis, Periodontal drug delivery system (PDDS), Nanoemulsion, Polydispersity Index, Zeta potential

How to cite this article: Rishabh Maurya, Ashu Mittal, Gaurav Tiwari (2026). Formulation, Optimization & Evaluation of Nanoemulgel Loaded with Roxithromycin and Eugenol for Effective Periodontitis Management. International Journal of Drug Delivery Technology; 2026;16(11s): 948-973. DOI: 10.25258/ijddt.16.11s.95

INTRODUCTION

significant prevalence and morbidity of periodontitis (PD), a serious public health issue, are linked to compromised masticatory function, poor dental oral health, and high dental treatment expenses (Tonetti et al., 2018, Sanz et al., 2020) [1-2]. Dental illness is the most widespread oral disease, striking up to 90% population of the world. Periodontitis impacts almost half of all US people aged 30 and over, and as many as 80% of adults have dealt with the disease at some point. Periodontal disease is a complex, multifactorial continual inflammatory response that impacts the adjacent hard and soft tissues. Gram-positive and gram-negative bacteria contribute to the more than 700 distinct "core" and "transient" microbial species that collectively make up the oral microbiome. (Deo et al., 2019) [3], which remarkably confer on the way to gingivitis, periodontitis and dental caries (Santosh et al.,

2021) [4]. Microorganisms, particularly gram-negative anaerobic bacteria, play a significant role in the development of periodontal disease. The presence of periodontitis is recognized by the examination of deeper periodontal pockets, loss of clinical attachment, and a decrease in alveolar bone, often alongside these signs. (Gandhi et al., 2025) [5].

The following factors contribute to this oral condition: smoking, obesity, certain drugs, poor brushing habits, and, finally, diseases like diabetes. (Jonesn et al., 2023) [6]. The development of biofilm-forming pathogens, namely, *Streptococcus mutans*, *Porphyromonas gingivalis*, *A. actinomycetemcomitans*, *Treponema denticola*, *Prevotella intermedia*, *Staphylococcus aureus* and *Escherichia coli* within the oral region habitat increases to microbial plaque origination on the surface and create other deformation around gingiva of the teeth and instigation of host-mediated inflammatory responses. Conventional treatments like scaling and root planning are ineffective for this bacterial accumulation in the periodontal pockets because they cannot reach deep within the pockets. Several of the preeminent usual signs related with gingivitis are bad breath, and bleeding, bright, tender or swollen gums (Yin et al., 2023) [7]. The depth of periodontal pocket is 3-5 mm of range. Both supra-bony and infra-bony periodontal pockets are forms of periodontal pockets (Maurya et al., 2019) [8]. Human teeth never change or remodel during the course of a lifetime, giving an intense and ongoing microbial colonization a non-shedding surface that makes periodontal therapy difficult (Maurya et al., 2024) [9].

A periodontal drug delivery system (PDDS) points to restore equilibrium by reducing the presence of these pathogens and enhancing patient health through non-surgical techniques, such as scaling and root planning, which can inspire confidence in alternative periodontal management methods. (Sanz et al., 2020) [10]. Given the connection between microorganisms and periodontal disease, it is advised to use local and/or systemic antimicrobials to manage the condition, improve infection control, reduce tissue damage from the immune response, and facilitate restorative healing. (Ilyes et al., 2024) [11].

Systemic antibiotics can penetrate periodontal tissues and efficiently address subgingival pathogens found in periodontal pockets, which might be challenging to reach using conventional mechanical cleaning methods. (Slots et al., 2002, Mehravani et al., 2024, Kapoor et al., 2012) [12,13,14]. Long-term use of antibiotics administered systematically can heighten the risk of developing antibiotic resistance and lead to negative drug reactions. (Loesche et al., 1996) [15].

Local Periodontal Drug Delivery Systems (LPDDS) encompass various methods of administering drugs aimed at preventing and treating oral illness. In the context of periodontitis, these local periodontal DDS act as supplementary cure options were beneficially utilized for managing the condition. By regulating the release of the drug, greater effectiveness and reduced harm effects can be attained. (Orive et al., 2003) [16].

As resistance to existing therapeutic agents grows among many common pathogens, there is a heightened interest in discovering new anti-infective drugs that incorporate natural compounds derived from plants. Roxithromycin (RXN), a semi-synthetic macrolide antibiotic with a 14-membered ring structure, is derived from erythromycin and exhibits both bacteriostatic and bactericidal actions by inhibiting protein synthesis and bacterial growth. Roxithromycin is known for its relatively broad spectrum of activity. However, RXN has an embittered taste and also less soluble in water. The 50% oral bioavailability and this low bioavailability is primarily attributed to its low solubility in water and lessen dissolution properties. RXN is effective against periodontal pathogens like *P. gingivalis* and *S. aureus* (Koopaei et al., 2012) [17].

Eugenol, the principal bioactive component of clove oil sourced from Eugenia aromatica, exhibits analgesic, anti-inflammatory, antibacterial, and local anaesthetic activities (Srivastava et al., 2016b; Ahmad et al., 2018a) [18, 19]. Molecular studies demonstrate that eugenol serves as an essential inhibitor of COX-2, while not affecting COX-1, thus clarifying its anti-inflammatory effects in murine macrophage cultured cells (Hong et al., 2002) [20]. Eugenol demonstrates capabilities of anti-inflammatory through the inhibition of cyclooxygenase-II, painkilling properties via selective binding to capsaicin receptors, and effect of antibacterial against monoderm and diderm bacteria (Jadhav et al., 2004) [21].

Nanoemulsions are lipid-contained drug delivery systems that contain a mixture of water, oil, cosurfactant, and surfactant with globule sizes ranging from 10 to 100 nm [22]. A liquid solution with pharmacokinetic stability is called a nanoemulsion. Compared to traditional formulations, nanoemulsions offer a number of benefits, such as improved medication solubility, easy penetration into the periodontal mucosa, dosage reduction, and fewer adverse effects. Surfactant and the outer membrane of microorganisms are fused in this nanodroplet, which kills the bacterium. The activity of nanoemulsion against bacteria is broad-spectrum. The tiny amount of detergent in the nanoemulsion formulation makes it safe for treating periodontal disease because it is selectively harmful to the microorganisms in concentration and does not irritate mucosal membranes. (Srivastava et al., 2014) [23].

Eugenol has been picked out as the drug and oil phase in the creation of the nanoemulsion. By circumventing its significant intestine and pre-systemic effect and extending occupancy of drug at the activity site, administration of

RXN locally to the buccal cavity has the prospective to maximise its local effect. Therefore, a very encouraging process for medicating periodontitis is to locally introduce roxithromycin in a systematic way although preserving its chemical stability and enhancing its solubility. (Nasra et al., 2017) [24].

Such treatments' clinical effectiveness is inherently dependent on the formulation's mechanical characteristics and drug release. Ideal formulations should therefore be decomposable, non-toxic, and non-irritating, have a long-acting release of the drug into the gingival crevicular fluid (GCF), be easy to inset in the periodontal pocket, and show hold within the pocket for the definitive amount of time (without the need for mechanical bonding to tooth surfaces). The gelling substance Carbopol 934P (CP 934P) was used for periodontal delivery. CP 934P interacts with the tooth and mucin-coated epithelium surfaces through certain interfacial forces in a process known as mucoadhesion, which is a particular type of bioadhesion. (Bruschi et al., 2009) [25].

Medicaments can now be delivered as liquid dosage forms using in-situ gel-forming formulations, which are a unique approach. Once applied at the delivery site, the pharmaceuticals form powerful gels, extending the active ingredient's residence time. Thermo-reversible and in-situ gelling systems are recognised as distinct technical approaches that transport medications straight into the pocket for regulated or prolonged release. (Garala et al., 2013) [26].

This research paper expresses the formulation development and characterisation of nanoemulgel affluence with eugenol as an oil phase and RXN medication used in periodontal pocket delivery for treatment of periodontitis. The central composite design was recruited to evaluate the roxithromycin-loaded eugenol nanoemulsion, which was optimised based on independent variables and also characterised by size of particle and PDI. Numerous characteristics, including capacity of gelling, pH, syringeability, antimicrobial study, in-vitro dissolution of drug and its kinetics and stability tests, were used to characterise the RXN NE gel.

2. Methodology

2.1 Materials

Roxithromycin was obtained from Yarrow Chem Products Pvt. Ltd., while eugenol had been attained by Loba Chemie Pvt. Ltd., also in Mumbai, India. Sun Pharma (Gurgaon, Haryana, India) supplied samples of Tween 80, Polyethylene Glycol (PEG), and other surfactants as a gift sample. The Milli-Q water purification system (Millipore, Bedford, USA) produced purer deionised water (DI). We procured and employed Carbopol 934P grades from CDH Chemicals Pvt. Ltd. in Mumbai, India.

2.2 Selection of excipients (oil, surfactant and co-surfactant)

Ensuring the drug remains dissolved is important for nanoemulsion stability, as low solubility can cause precipitation. Excipients were prefered based on solubility, miscibility, and stability. The selected surfactants included Tween 80, Tween 20, Peceol, Labrafil, and Labrasol. Polyethylene glycol (PEG-400) and ethanol were considered as co-surfactants, and eugenol (EUG) was pick out as both the oil phase and the active ingredient. To study the interaction between the drug (RXN) and the solvents (oil, surfactant, and co-surfactant), the maximum amount of RXN was added. One milliliter of each selected solvent was placed in microcentrifuge tubes and shaken at 25 ± 1ºC for 72 hours using the shake flask method. After shaking, undissolved drug was removed by centrifuging at 4000 RPM for 10 mins. The supernatant was then filtered through a 0.45 mm nylon membrane. Various dilutions of the filtered supernatant were prepared, and the drug concentration in the oil or surfactant was measured using an already progressed calibration curve at 205 nm with a UV-spectrophotometer (Systronics Double Beam-2203).

The maximum amount (RXN) dissolved with 1 ml of surfactant in a microcentrifuge tube and vortexed at 25°C for 72 hours using a Apex Labs-101 cyclomixer. After 72 hours, any undissolved drug was removed by centrifuging the mixture at 3000 rpm for 10 minutes with a Remi R8C Laboratory Centrifuge. Then, 10 µL of the supernatant was shifted to a microcentrifuge tube and adulterated to 1 mL methanol. The solution was vortexed again and filtered through a 0.45 mm nylon membrane filter. Various dilutions of the filtered supernatant were prepared, and the concentration of the drug in oil or surfactant was quantified using a previously developed calibration curve at 205 nm absorbance. The solubility of the drug in different excipients was determined first, led by a study of stability of the prepared nanoemulsion.

2.3 Preferable selection of formulations

Formulations were selected from each created phase diagram according to the ensuing specification:

- 10 mg was selected as the dose for developing the nanoemulsion because the approved daily dose ranges from 150 to 300 mg.
- The oil concentration should be sufficient to readily dissolve 100 mg of the drug.
- For each oil percentage chosen, the formula was based on the phase diagram. This diagram identified the lowest Smix concentration for nanoemulsion formation.

2.4 Development of pseudo ternary phase diagrams

A nanoemulsion was formulated using either the method of aqueous titration or the spontaneous emulsification method.

Eugenol was then selected as the oil phase following a solubility screen; its therapeutic profile predisposed it to be an ideal component of the nano-emulsion. Surfactant/Co Surfactant Pairing, PEG 400 (co-surfactant) and Tween 80 (surfactant) were chosen due to their high emulsifying ability while distilled water served as the aqueous phase. Phase diagram Construction were prepared using the Aqueous-Phase Titration or spontaneous emulsification methods to determine the nanoemulsion zone. Different ratios of S_{mix} (surfactant: co-surfactant) were experimented with 1:1, 1:2, 2:1, 3:1, 4:1, 5:1, 6:1, 7:1. These S_{mix} proportions were adjusted to escalate the surfactant concentration relative to the co-surfactant and vice versa, allowing for a thorough review of the phase diagram. The oil was mixed thoroughly with specific S_{mix} ratios in proportions differing from 1:9 to 9:1 for each phase diagram. 16 different oil: S_{mix} mixtures were made to cover the entire design space (1:9, 1:8, 1:7, 1:6, 1:5, 1:4, 1:3, 1:2, 2:8, 3:7, 4:6, 5:5, 6:4, 7:3, 8:2, and 9:1) to ensure comprehensive coverage of potential ratios and validly define the phase borderlines. Phase Diagram Construction by Aqueous-Phase Titration, addition of water to the oil: Smix mixture was carried out gradually until the mixture turned turbid or phase-separated.

The nanoemulsion zone was delineated by 3 axis plot, X axis: Oil concentration, Y-axis: concentration of aqueous (water), and Z -axis: S_{mix} concentration (fixed ratio per plot). The S_{mix} (proporation) ratio stayed constant. The zone of nano-emulsion occurs in the form of a specific contiguous segment of stable emulsion of clear appearance, which varies in size and shape depending on the selected S_{mix} ratio and technique.

2.5 Formulation of a nanoemulsion containing Roxithromycin and eugenol

The RXN nanoemulsion was formulated employing the spontaneous emulsification method. The drug was diffused in the oil phase (Eugenol) to acquire a homogeneous solution. This drug-oil mixture was then combined with a pre-mixed surfactant and co-surfactant system (S_{mix}) and homogenized at 1500 rpm to form the organic phase. A measured volume of the phase of aqueous was added dropwise to the organic phase under continuous stirring to form an oil-in-water (o/w) emulsion. Subsequently, the aqueous phase was separated by evaporation under reduced pressure, resulting in the formation of a nanoemulsion.

2.6 Election to optimize nanoemulsion formulation employing response surface modeling

A Box–Behnken approach featuring three factors, three levels was waged via Design Expert software (ver. 13.0.5.0, Stat-Ease Inc., Minneapolis) to examine the quadratic response surface & develop polynomial (algebraic) equating for the optimisation of the nanoemulsion formulation. Table 1 presents the variables that were chosen alongside their corresponding low, medium, and high levels. A numerical assessment was conducted for assessing the chief, interrelation, and quadratic effects of the specified variables on important response parameters, which include the size of particles, polydispersity index (PDI), and zeta potential. The design matrix, as conferred in Table 1, comprised a total of 17 experimental runs. The nonlinear quadratic model that was the result of the analysis of variance is in the form and observe:

$$Y=b0 + b2X1 + b2X2 + b3X3 + b12X1X2 + b13X1X3 + b23X2X3 + b11X12 + b2X22 + b33X32 \quad (1)$$

In the polynomial analysis, Y represented the measured response for each combination of factor levels, b0 indicated the intercept, and b_1–b_{33} were the regression coefficients derived from the experimentally recorded values of Y. The variables X_1, X_2, and X_3 represent the coded levels of the explanatory (independent) variables, and their corresponding interaction and quadratic terms were included in the design (Govender et al., 2005, Chopra et al., 2007) [27]. The numerical robustness of the polynomial (algebraic) equations initiated by Design-Expert was confirmed through the use of analysis of variance (ANOVA) by the software. Furthermore, the adequacy of the model was assessed by examining the statistical significance of the coefficients and the (R^2) values.

Table 1. Optimization of the RXN nanoemulsion formulation through the supplication of response surface methodology (RSM)

S.No.	Factor Independent variable (% v/v)	Conc. Scrutinized	Level used		Optimized Value
			Low (-)	High (+)	
1	X_1= (Conc. of oil phase)	10–16	10	13	16
2	X_2= (Surfactant: co-surfactant ratio) S_{mix}	30–45	30	37.5	45

3	X_3= amount of water	50–60	50	55	60
	Response variable	Optimization Aim			
4	Y_1= Globule size (nm)	(↓) Decrease			
5	Y_2= Polydispersity Index (PDI)	(↓) Decrease			
6	Y_3= Zeta potential (mV)	(↑) Increase			

2.7 RXN Nanoemulsion Physical Testing for Stability

Physical stability tests were conducted to address issues associated with the metastability of nano-formulations. The physical stability of the nanoemulsion formulations is critical to its overall performance, as it can be compromised by drug (crystallization) precipitation within the excipient matrix. Besides, deficient physical stability may produce effects in phase separation of the excipients, which could negatively impact both the functional performance and the visual appearance of the formulation. (Shafiq et al.,2007) [28].

2.7.1 Centrifugation study

The developed nano-formulations were put through to centrifugation at 5000 rpm for 30 minutes to evaluate physical stability, specifically for indications of phase separation, creaming, or cracking. Formulations exhibiting no detectable instability under these conditions were subsequently selected for further assessment via a heat–cooling cycle.

2.7.2 Cycle of Heating–cooling

The experiments were designed to assess the impact of temperature fluctuations on nanoemulsion stability. Each selected formulation underwent six heat–cooling cycles, between 4°C and 40°C, with a minute holding span of 48 hours at each temperature. Stability was assessed after the completion of these cycles, and only those formulations maintaining stability were advanced for further evaluation through freeze–thaw cycle testing.

2.7.3 Cycle of Freeze thaw

The formulations went through thrice cycles of freeze-thaw, with temperatures ranging from 2ºC to 25ºC. Each temperature was maintained for at least 48 hours. Only the formulations that proceeded the test which was selected for the study of dispersibility to measure how efficiently they dispersed. (Bali et al., 2010) [29]

2.8 Characterization of Nanoemulsion Formulations

2.8.1 Determination of Globule size and Index of Poly Dispersity

Spectroscopy of Photon correlation, which is based on the theory of dynamic light scattering (DLS), to find out the average size and polydispersity index (PDI) of the nanoemulsion droplets. In DLS, a laser beam shines on a sample inside a cell, and the light's intensity that is dispersed by the particles changes at a frequency that depends on the size of the particles. The diffusion coefficient of the particles may be found by looking at these changes, and then the size of the globule can be found. We did all of the measurements after diluting the material by up to 100 times and keeping the temperature at 25°C. To make sure the results could be repeated, each experiment was done three times. (Belhaj et al., 2012) [30]

2.8.2 Potential of electrokinetic Determination

The nanoemulsion (0.1 mL) was first diluted 100-fold with double-distilled water to a final volume of 10 mL. Zeta potential measurements were then performed at 25 °C using a Malvern Zetasizer equipped with a 4 mW He–Ne laser (633 nm). The instrument can resolve potentials from –120 V to +120 V. In colloidal science, a zeta potential of ±30 mV or higher is generally considered to confer strong electrostatic stability. All of the improved formulations displayed negative zeta potentials, confirming that they possess a net negative surface charge and are therefore electrostatically stabilized. Furthermore, a comparative evaluation with particle size data disclosed that a depletion in droplet size was generally equated with a decrease in the magnitude of the negative surface charge.

2.8.3 Determination of Structure of Surface by TEM Analysis

Transmission electron microscopy (TEM) was utilized for the external surface features of the internal phase. The emulsion was thinned to a concentration of up to 100 times, and the drop of the diluted sample was meticulously lay down onto a grid of copper (300-mesh), sit aside for one minute. The grid was then turned over, a drop of (PTA) phosphotungstic acid was appealed for a duration of 10 seconds as a negative stain. Excess stain was gently absorbed using filter paper, and the prepared grid was subsequently assessed under a transmission electron

microscope (JEOL, Model JEM 1011) for structural assessment. (Srivastava et al., 2016) [31].

2.9 Preparation of RXN Nanoemulsion Gel/ Nanoemulgel (NEG)

Nanoemulsions generally exhibit lower viscosity compared to gels, which may limit their period of residence at the application area. For effective drug delivery, the formulation must remain localized until optimal drug penetration is achieved. In the case of gingival tissues, viscosity plays a critical role in both permeation and prolonged retention of the drug. Therefore, Carbopol 934P was incorporated as a gelling agent to escalate the viscosity of the nanoemulsion, thereby improving its ability to remain at the site of application. This modification facilitates finer retainment of the nanoemulsion-based gel on periodontal site. (Hosny et al., 2013, Mahmood et al., 2023) [32, 33]. Carbopol is widely recognized as a safe, non-irritant gelling agent, and to date, no reports have indicated any harm reactivity or adverse reactions associated with its topical application in humans. (Mahmood et al., 2023, Ahad et al., 2017) [33, 34]. Carbopol 934P (17.5 % w/v) was first dissolved in distilled water with the aid of a mechanical stirrer and subsequently stored at 2-8ºC for a duration of 12 hours to guarantee thorough wetting (cold method). The optimized nanoemulsion was incorporated into the sol system (hydrogel base) and maintained at 4ºC for a duration of 24 hours, resulting in the formation of a nanoemulgel.

2.10.1 Evaluation of Roxithromycin laden nanoemulgel

2.10.1.1 Determination of pH of Nanoemulgel

The pH of RXN loaded nanoemulgel (NEG-9) should correspond to the pH of the saliva and SGCF (5.5–8.0) therefore, 0.5 g sol was diluted in the 50 ml distilled water and stored at 4ºC. The pH of the preferred nanoemulgel (NEG-9) was conducted by digital pH meter (Labix Industries, model LBX-505). The test was implemented in triplicate and mean value was reported. (Al-Suwayeh et al., 2014) [35].

2.10.1.2 Measurement of transition of Sol-gel

Determining the sol-gel transition temperature of a periodontal formulation with the test-tube inversion technique. (Kumari and Pathak et al., 2012) [36]. Consisely, 5 mL of the sol was transferred into test tubes, sealed with aluminum foil, and submerge in a thermostat-controlled water bath initially set at 4°C. The temperature was then gradually increased in accretion of 0.5°C, allowing the sol to equalize for 1 minute at each step. Gelation was considered to have arisen when the meniscus remained immobile as slant manner in the tube to a 90° angle, and the corresponding temperature was observed as the gelling temperature. For gelling time determination, 5 mL of the sol was maintained at 37°C in a water bath, and the time required for gel formation was measured. All observations were executed in triplicate.

2.10.1.3 Syringeability

The syringeability of the RXN-laden nanoemulgel was tested by a 1 mL plastic syringe equipped with a 22-gauge needle. A specific volume of the formulation, kept at 4°C in a sol state, was placed into the syringe, and uniform, gentle pressure was pertained to the plunger. Precautions were taken to prevent the inclusion of air bubbles during this process. The assessment of syringeability was conducted qualitatively.

2.10.1.4 Homogeneity test

The formulations were subjected to visual inspection for the presence of particulate matter or aggregates. Based on appearance, they were categorized into three grades: A+ (good), A (fair), and A– (poor). Furthermore, a minute sample of RXN nanoemulgel was compressed between the thumb and index finger to qualitatively evaluate consistency and to confirm the homogeneity of the formulation. (Ahad et al., 2017) [34].

2.10.1.5 Spreadability Study

The nanoemulgel's spreadability (NEG-9) was analyzed by placing 0.5 gm of the RXN nanoemulgel within a defined circle of 2 cm diameter on a glass plate. A second glass plate has placed atop the first and weighed down with an additional 0.5 kg for a duration of 5 to 6 minutes, during which an increasing the diameter after spreading was seen. The characteristics of gel spreadability demonstrated little time for dispersion and exhibited consistency. (Balap et al., 2024) [37].

$$\text{Spreadability (S)} = M \times L / T \qquad \text{eq. (2)}$$

S = spreadability measured in grams per second.
M = stands for mass, expressed in grams
L = denotes the length of the slide, giving us an understanding of the distance involved.
T = time measured in seconds.

2.10.1.6 Extrudability test

Extrudability is defined as the facility with which a semisolid formulation can be expelled from its container (e.g., tube or pump) under applied pressure, without requiring excessive force or causing blockage. To evaluate extrudability, 10 g of the nanoemulgel formulation was transferred into collapsible aluminium tubes, which were subsequently sealed by crimping the ends. The filled tubes were weighed accurately, kept link two glass slides, and

subjected to a uniform load of 500 g. Following removal of the cap, the extruded gel was assembled and weighed. The extrudability was intimated as the % of formulation expelled relative to the total content. Formulations demonstrating more than 90% extrudability were classified as excellent, those with more than 80% as good, and those exceeding 70% as fair. (Kandale et al., 2023) [38].

2.10.1.7 Differential Scanning Calorimetry (DSC) of the RXN Nanoemulgel

A Mettler Toledo DSC -1 Star was used to investigate the thermal behaviour and possible drug-excipient interactions of a pure roxithromycin sample and the RXN nanoemulgel formulation. These were to identify the melting point of the drug, test its thermal stability, and identify any endothermic or exothermic reactions that could occur between the drug and formulation excipients. The 6 mg sample was progressively heated from 30 to 300ºC. A continual flow of nitrogen (60 mL/min) has maintained, while the temperature was expanded at a rate of 10ºC/min. (Shaikh et al., 2009, Cordeiro et al., 2023, Hafez et al., 2015, Gupta et al., 2019) [39-42].

2.10.1.8 Measurement of Rheology of Nanoemulgel

Rheology is a censorious criterion in evaluating the flow characteristics of semisolid dosage forms. In this study, the viscosity of the selected gelling agent as well as the optimized nanoemulgel formulation was determined at three different temperatures (4°C, 25°C and 37°C). Measurements were performed using a Brookfield viscometer (BBAU, Lucknow) equipped with spindle LV-4, which was immersed perpendicularly into the sample and rotated at controlled shear rates corresponding to spindle speeds of 10, 20, and 50 RPM. The viscosity values obtained at each rotational speed were recorded. The experimental data were further analyzed using RHEO V.2.8 software (Brookfield engineering labs), and fitted to various rheological models. Among the tested models, the Herschel–Bulkley model provided the best fit, indicating that it appropriately expressed the flow behaviour of the optimized nanoemulgel formulation.

$\tau = \tau_0 + ky^n$ --------eq. (3)

τ = shear force

τ_0 = yield value

k = index of consistency

y = rate of shear

n = index of flow behavior

2.10.1.9 Percentage Content of Drug Determination

Content of drug Determination was performed by exactly weighing (10 mg) nanoemulgel (NEG) formulation, dissolving in methanol (10 mL) of under continuous stirring using a vortex mixer. The developing solution has filtered through Whatman filter paper (grade 41) to remove particulate matter. Following appropriate dilutions, the concentration of roxithromycin (RXN) in the NEG formulations was calculated by UV–Visible spectrophotometer at 205 nm.

2.10.1.10 Test of *in-vitro* drug dissolution and the release kinetics of NEG with RXN

These investigations were conducted utilizing the dialysis bag diffusion technique. A total of 400 mg of 2% drug of periodontal gel was introduced into a pretreated dialysis membrane (MWCO 6000–8000 Da), which had been hydrated in simulated gingival crevicular fluid (SGCF, phosphate buffer, pH 6.8, formulated to mimic the pathological pH conditions related to periodontal disease) for 48 hours prior to the experiments. The dialysis bag was submerged in 100 mL of SGCF, retained at a constant temperature of 37±0.5°C while being agitated constantly at 100 rpm. At designated intervals (0, 0.25, 0.5, 1, 2, 3, 4, 5, 6, 7, 8, 12, and 24 hours), samples of the release medium were taken and supersede with fresh SGCF to maintain sink conditions. The quantity of RXN released assessed using a validated UV–visible spectrophotometric method at a wavelength of 205 nm.

2.10.1.11 Analysis of *Ex-vivo* Skin Penetration in dermal

Ex-vivo penetration experiments were performed with the use of goat buccal mucosa as a barrier membrane. Buccal tissues were obtained fresh at a nearby abattoir and immediately brought to laboratory in chilled normal saline. The epithelial layer was dissected with utmost attention and used not later than 2 h of excision. The washed buccal mucosa was cut into fragments of about 3×2 cm and put at the start between the donor and receptor compartments in Franz Diffusion Cell (FDC). Phosphate buffer saline (PBS, pH 6.8), 1 mL of imitated gingival crevicular fluid (SGCF), was added to the receptor chamber, and the optimum ROX nanoemulgel formulation (NEG-9, which is equivalent to 1 mL) was added to the donor chamber. The experiment was done with controlled conditions and aliquots were taken at specific intervals during the experiment period of 6 h. The value of the concentration of roxithromycin that passed across the membrane was determined at 205nm using the UV- visible spectrophotometer (Systronics 2203).

The permeation profile has revealed not more than 50% of the drug diffused across the buccal mucosa, with the majority hold on to the tissue. This outcome suggests that the nanoemulgel facilitates site-specific drug retention within the buccal epithelium, thereby offering localized therapeutic action while minimizing systemic absorption. Such targeted delivery not only enhances therapeutic

efficacy but also lessen the likelihood of side effects in bloodstream and antimicrobial resistance.

2.10.1.12 Determination of *Ex-vivo* force of mucoadhesion

Mucoadhesive strength detect by texture analyzer (TA-XT plus, Stable Micro Systems, Surrey, UK) was employed on formulated nanoemulgels (NEGs) with differing polymer concentrations. We obtained freshly excised goat buccal mucosa and immediately immersed it in simulated gingival crevicular fluid (SGCF, pH 6.8) at 4°C. Prior to use, the tissue was rinsed with ice-cold PBS and sectioned to a thickness of 2.0–2.3 mm. All experiments were performed within 2 hours of tissue collection at three specific temperatures (4, 25, and 37°C). For each measurement, 50 mg of the gel was uniformly distributed over an area of 2.41 cm^2 on the mucosal aspect of the buccal membrane. A pre-load of 25 g was administered for 10 seconds to facilitate the adhesion of the gel to the mucosa. Once the pre-load was removed, the probe was utilized to exert a detachment force until the two components separated. The maximal force required to detach the two components was termed mucoadhesive strength (MS). Each experiment was conducted three times (n = 3), yielding statistically significant findings at $p \leq 0.05$. (Bruschi et al., 2007, Sharma et al., 2012) [43, 44]

2.10.1.13 Antibacterial Activity

Both the antibacterial activity of eugenol gel and a nanoemulgel (NEG) loaded roxithromycin was done using the agar well diffusion method (cup-plate technique). The test organisms were selected as *Staphylococcus aureus* and *Escherichia coli*. As the growth medium used in the antibacterial assessment, nutrient agar was used. New broth cultures of both bacteria were inoculated to contain a turbidity of approximately 10^8 CFU/mL. The sterile petri dishes were inoculated with sterilized molten nutrient agar and allowed to dry. After solidification, 100 µL of the microbial suspensions which had been standardized was aseptically inoculated on the surfaces of the agar. A 5 mm agar plate uniform wells were aseptically constructed in the agar at equal distance using a sterile cork borer. The wells were then added with the test formulations and then the plates were grown at 37±0.5ºC in 48 hours. The incubation was followed by measuring the diameter (in mm) of the zones of decreiment surrounding each of the wells to assess the antibacterial effectiveness. All observations were assessed in triplicate (n=3) to ensure reproducibility.

2.10.1.14 Stability Studies of Optimized Nanoemulgel

The stability of the semisolid nanoemulgel formulation was assessed over a duration of 3 months. The optimized formulation was kept under various conditions: at 5ºC, 25ºC, 40ºC, and 75% relative humidity (RH), as well as at room temperature. The samples were evaluated at 15-day intervals in terms of the organoleptic properties, physical stability, viscosity, and spreadability. (Sohail et al., 2018, Ullah et al., 2023) [45, 46]

3. Result & Discussion

3.1 Screening of excipients (oil, surfactant and co-surfactant)

In this research, eugenol act as the oil phase owing by superior solubilizing capacity for the drug. Among the evaluated surfactant–co-surfactant (S_{mix}) systems, the combination of Tween 80 (surfactant) and, polyethylene glycol (PEG-400, co-surfactant) yielded the highest nanoemulsion region (29.20%) as shown in Figure 1. Tween 80, with a hydrophilic–lipophilic balance (HLB) value of 15.0, demonstrated efficient emulsification, while PEG-400 further enhanced solubilization.

The relatively low molecular weight of Tween 80 was advantageous in reducing droplet size more effectively compared to higher molecular weight polymeric surfactants. Following the drug disclosed maximum solubility in eugenol, and chosen as the oil phase for nanoemulsion formulation. Moreover, the combination of Tween 80 and PEG-400 as surfactant and, co-surfactant, produced a transparent and stable nanoemulsion system, confirming their suitability for formulation design.

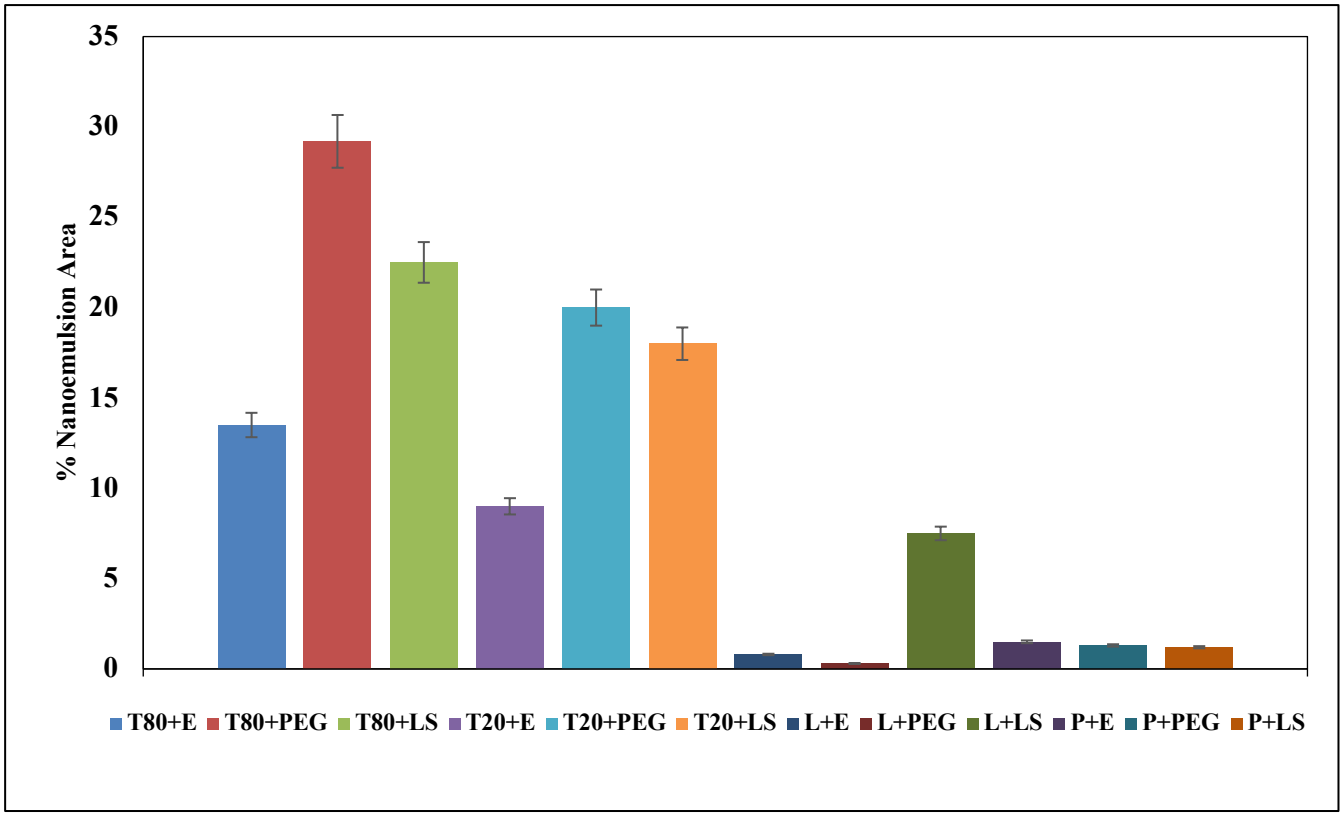

Fig.1.Percentage of area of nanoemulsion achieved using different surfactant–co-surfactant combinations.

3.2 Development of Nanoemulsion phase diagrams

Pseudo-ternary phase diagrams were developed by ternaryPlot.com software online to evaluate different S_{mix} ratios. The analysis demonstrated that variations in the surfactant-to-co-surfactant ratio influenced the isotropic nanoemulsion region, which was primarily dependent on the capacity of S_{mix} to solubilize the oil phase. As illustrated in Figure 2, the S_{mix} ratio of 1:1 produced a comparatively larger nanoemulsion region than the 1:2 ratio, where a higher proportion of PEG-400 led to a reduction in the emulsification area. The nanoemulsion region increased progressively up to an S_{mix} ratio of 6:1; however, further increase to 7:1 resulted in a reduction, possibly due to insufficient co-surfactant content to maintain efficient emulsification.

From these observations, the 6:1 S_{mix} ratio was identified as the most suitable for nanoemulsion development, as it generated the broadest nanoemulsion region, verified by both visual assessment and the cut & method. The final NEG formulation, eugenol was adopted as the oil phase, with an optimized oil-to-S_{mix} ratio of 1:4.

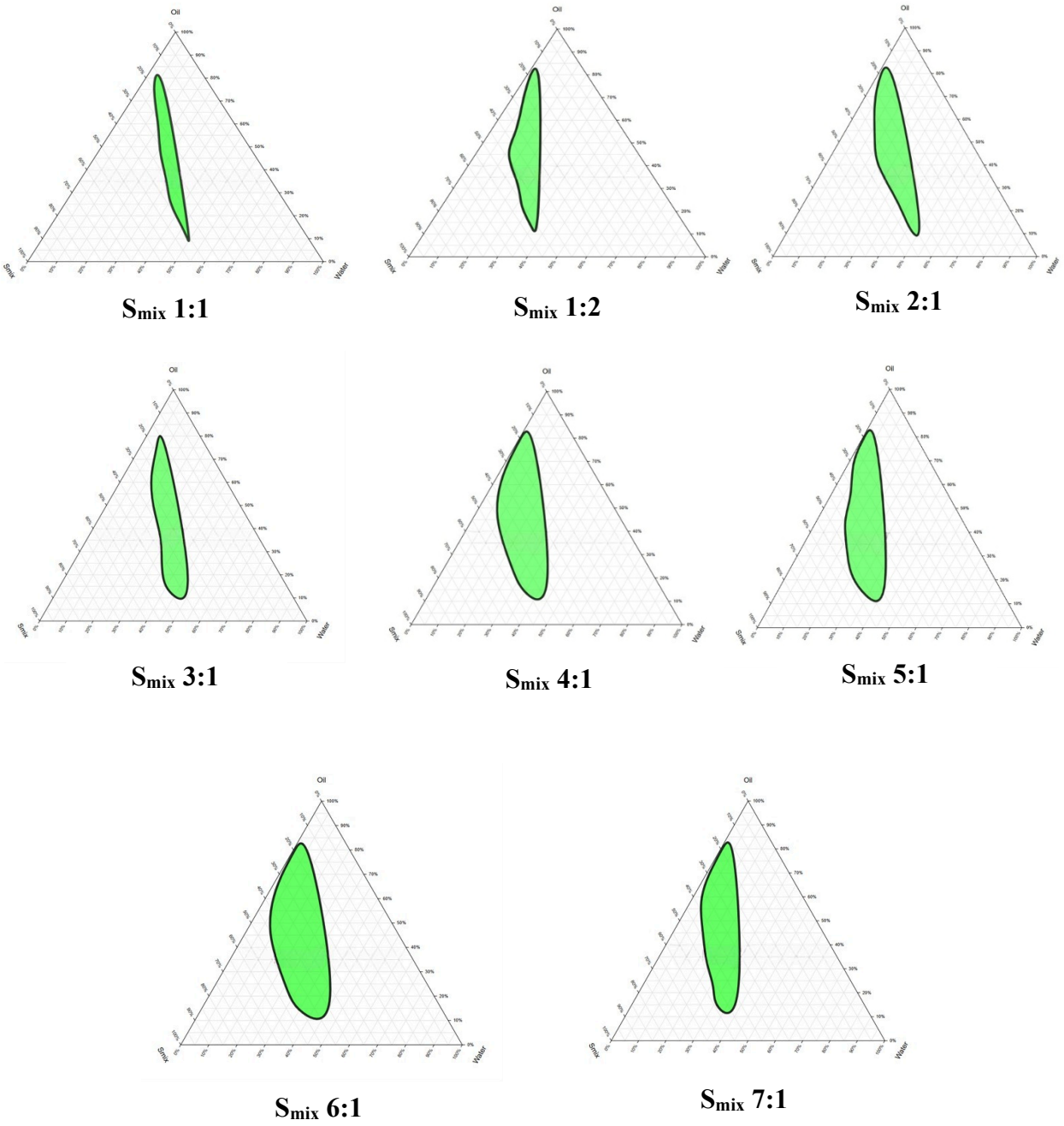

Fig. 2. The pseudo-ternary phase diagrams were created featuring Eugenol (as the oil phase), Tween 80 (serving as the surfactant), and PEG-400 (acting as the co-surfactant). The colored regions in the diagrams denote the area of oil-in-water (O/W) nanoemulsion, which was achieved at different ratio (1:1, 1:2, 2:1, 3:1, 4:1, 5:1, 6:1 and 7:1) of surfactant to co-surfactant (S_{mix}).

3.3 Statistical Optimization of Nanoemulsion Parameters Using Response Surface Methodology

3-factor with 3-level Box–Behnken numerical approach was utilized to optimize the NEG formulation, necessitating a total 17 experimental trials. The responses recorded (Y_1, Y_2, and Y_3) throughout all trials were determined to be within the ranges of 34.6 ± 0.21 to 86.19 ± 0.36 nm, 0.185 ± 0.002 to 0.468 ± 0.004, and –14.56 ± 0.34 to –29.54 ± 0.44 mV, respectively (Table 2). The experimental data for all 17 formulations were evaluated using linear, two-factor interaction, and quadratic models. The quadratic model yielded the optimal fit for all three replies (Y_1, Y_2, and Y_3).

Table 2. Box–Behnken design of experimental outlining the selected factors and corresponding responses obtained for robustness evaluation.

Formulation Code	Independent variables			Dependent variables		
	Factor A: (X_1) Oil (ml)	Factor B: (X_2) S_{mix} (%)	Factor C: (X_3) Water (ml)	Response1: (Y_1) Particle size (nm)	Response2: (Y_2) PDI	Response3: (Y_3) Zeta Potential (mV)
NEF1	13	37.5	55	34.6	0.213	-28.37
NEF2	13	37.5	55	36.24	0.214	-28.38
NEF3	10	37.5	60	35.1	0.189	-29.54
NEF4	10	45	55	50.51	0.319	-22.21
NEF5	13	45	60	54.51	0.339	-21.21
NEF6	16	45	55	60.57	0.341	-19.71
NEF7	13	30	60	82.42	0.451	-16.34
NEF8	13	37.5	55	35.18	0.215	-28.56
NEF9	13	45	50	50.21	0.336	-21.5
NEF10	16	37.5	50	37.22	0.24	-26.74
NEF11	13	37.5	55	36.11	0.216	-28.39
NEF12	16	30	55	83.55	0.468	-14.56
NEF13	13	37.5	55	36.24	0.214	-28.5
NEF14	10	30	55	85.09	0.41	-17.93
NEF15	10	37.5	50	36.11	0.185	-29.11
NEF16	13	30	50	86.19	0.461	-16.82
NEF17	16	37.5	60	37.19	0.226	-25.66

3.3.1 3D graphs and response surface methodology were employed to optimize the nanoemulsion formulation based on particle size, polydispersity index (PDI), and zeta potential

The 3-dimensional contour graphs and response surface were assessed as depicted in Figure 2.

3.3.1.1 Outcome of independent factors on particle size

Particle's size plays a key role in the assessment of nanoemulsions. A decrease in particle size leads to an enlarge in the interfacial area of surface, which improves the efficiency of absorption of drug. According to Equation (4), the Model F-value of 1132.98 demonstrates the relevance of the Model. The likelihood of obtaining such a "Model F-value" uniquely by possibility is only 0.01%. "Prob>F" values lower than 0.0500 imply that the Model terms are statistically significant. In this context, the Model variables X_1, X_2, X_1X_2, X_{12}, and X_{22} were originate to be prominent. Greater the values than 0.1000 suggest that those Model variables lack significance. When compared to pure error, a deficit-of-fit rating of 1.36 indicates that the degree of lack of fit is not substantial. The chance of observing this "lack of fit F-value" due to random variation is 37.37%. The predicted R^2 value of 0.9984 is closely matched with the adjusted R^2 value of 0.9939. The ratio of 84.461 suggests a sufficient signal (Table 3). This result framework provides as a tool for inspecting the design space effectively. Adequate precision evaluates the relationship between the signal and the noise present. A ratio greater than 4 was deemed advantageous. Our data proves augmenting the concentration of S_{mix} first diminishes the particle size of the nanoemulsion to a specific threshold. However, beyond that point, additional increments in S_{mix} concentration tend to increased particle sizes. Furthermore, fluctuations in oil and water concentrations didn't determine size of particle.

$$Y_1(\text{ParticleSize})=+35.67+1.16X_1-15.39X_2 \quad 0.1650X_3+2.78X_1\ X_2+0.2450X_1\ X_3+ \quad 2.22X_2\ X_3+1.21X_1^2+32.93X_2^2-0.475X_3^2 \quad (4)$$

3.3.1.2 Outcome of independent factors on PDI

The PDI functions as a quantitative procedure, providing insights into the similarity of particle size distribution with a specified framework. Table 2 indicates that all the nanoemulsions exhibited a lean range of size distribution. The F-value of 16912.28, as displayed in Equation (5), indicates that the model is credible. The likelihood of attaining a "Model F-value" of this magnitude via random fluctuations is only 0.01%. P-values below 0.0500 signify that the model terms are deemed highly significant. The model includes significant terms: X_1, X_2, X_3, X_1X_2, X_1X_3, X_2X_3, X_1^2, X_2^2, and X_3^2. Values exceeding 0.1000 indicate that the corresponding model variables lack prominence. When many model variables was inconsiderable, except for those essential to maintain structure, pursuing model reduction may enhance the complete efficiency of the model.

Its deficit-of-fit F-value of 0.58 is insignificant compared to the pure error. There is a 66.03 probability of the lack of fit F-value of this size as a result of random noise. The expected value of R^2 is 0.9997 which is similar to the corrected R^2 of 0.9999. The ratio of 359.407 signifies an suitable signal, as demonstrated in Table 3. This model functions as a tool for investigating the design space, with adequate precision quantifying the relationship between signal and noise in the data, aiming for a desired ratio exceeding 4. Our conclusions demonstrate that an enlarge in concentration of S_{mix} reduces the nanoemulsion PDI to a specific threshold; beyond this threshold, additional increases in S_{mix} concentration result in an increase in PDI. A higher oil concentration outcomed in an increased PDI value; nevertheless, its result was smaller noticeable compared to that of S_{mix}.

$$Y_2 \text{ (PDI)} = +0.214+0.024X_1-0.056X_2-0.003X_3-0.007X_1X_2+0.005X_1X_3+0.006X_2X_3-0.007X_1^2+0.176X_2^2+0.002X_3^2 \quad (5)$$

3.3.1.3 Outcome of independent factors on (electrokinetic) Zeta Potential

It suggests the existence of a repulsive force among neighboring particles with identical charge in the dispersion. The Model F-value of 6699.28, as shown in Equation (6), highlights the significance of the model. The probability of obtaining a "Model F-value" of this magnitude due to random chance is exceedingly low, at 0.01%. The model is statistically significant, as the "Prob>F" values were below 0.0500. The most significant names identified in the model include X_1, X_2, X_1X_3, X_2X_3, X_{12}, X_{22}, and X_{32}. Values greater than 0.1000 were suggested as indicators of the insignificance of the framework terms. The lack-of-fit F -value of 1.00 indicates that the lack-of-fit is insignificant relative to pure error, with a 48.05 probability of random variation giving such a lack-of-fit F -value. The adjuster R^2 of 0.9997 is consistent with the value of predicted R^2 of 0.9991. The ratio of 229.613 indicates a strong signal (refer to Table 3). The established framework serves as an effective tool for exploring the design space. Reasonable precision evaluates the correlation between signal and noise, favouring a ratio greater than 4 in this analysis.

Research findings stipulate that an enlarge in S_{mix} concentration leads to a the nanoemulsion's negative zeta potential is higher, up to a point, after which further increases in S_{mix} concentration result in a lower in negative zeta potential. The shifts in water and oil zeta potential showed no discernible effect of concentration.

The numerical optimisation methodology was occupied to improve the nanoemulsion. The refined formula was developed after a comprehensive analysis of the impact of independent variables on the responses. The norm applied in originating the optimised solution entailed the meticulous selection of individual variables and the definition of their corresponding limits and target ranges. Table 1 presents the optimisation limitations identified for each variable. The optimised nanoemulsions attained the preferred nanosize range (see Figure 3), exhibiting a low polydispersity index (PDI), a high zeta potential (refer to Figure 4), thereby effectively inhibiting aggregation. The zeta potential is an essential aspect in determining the stability of dispersions within colloidal systems. Table 4 demonstrates a significant correlation between the forecasted and experimental values ($p \leq 0.05$), suggesting a high level of accuracy in the predictions generated by Design Expert. This underscores the effectiveness of the experimental design in tuning the nanoemulsion to meet the specific requirements.

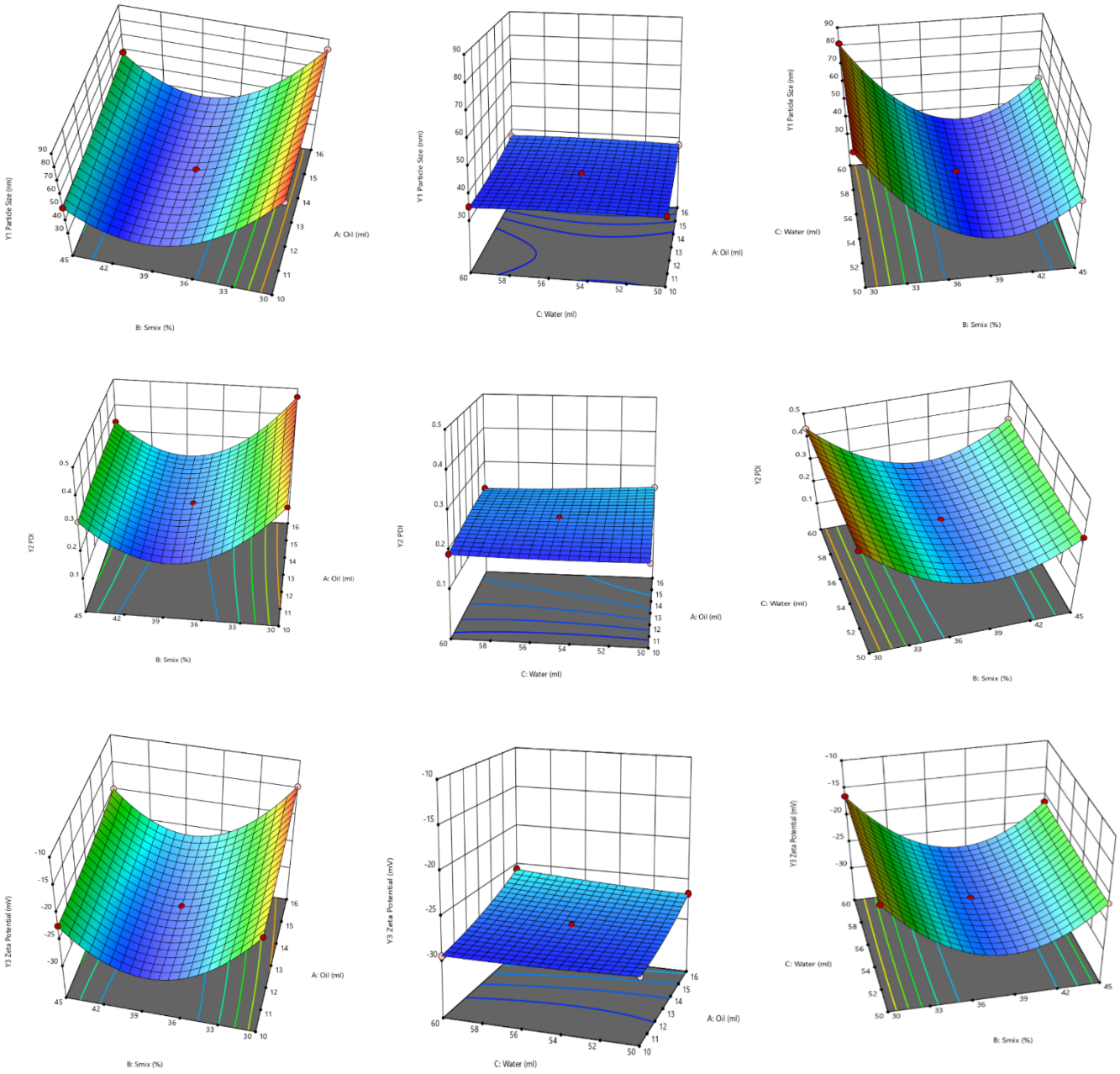

Fig. 3. Three-dimensional response surface plots illustrating how varying quantities of oil, S_{mix} (Tween 80: PEG 400), and water impact the size of particle, polydispersity index (PDI), and zeta potential of the nanoemulsion.

Table 3. ANOVA evaluation of experimental design responses (Y_1, Y_2, and Y_3)

Response	Model	F value	p value Prob>4F	Implication	R^2	Adjusted R^2	Predicted R^2	Adeq precision
Y_1 (Particle size)	Quadratic	1132.98	< 0.0001	significant	0.9993	0.9984	0.9939	84.4614
	Unsuitability	1.36	0.3737	Not significant				

Y_2 (PDI)	Quadratic Unsuitability	16912.28 0.5769	< 0.0001 0.6603	significant Not significant	1.0000	0.9999	0.9997	359.4072
Y_3 (Zeta potential)	Quadratic Unsuitability	6699.28 0.9954	< 0.0001 0.4805	significant Not significant	0.9999	0.9997	0.9991	229.6125

Table 4. The optimized nanoemulsion formulation was evaluated to equate the predicted values with the experimental results obtained using the optimized composition generated by (DOE) Design-Expert® software (version 13.0.5.0)

Optimized component	Optimized quantity	Dependent variable	Forecasted value	Observed value
Oil (%)	13.0	Size of Particle (nm)	49.673	50.21
S_{mix} (%)	37.0	PDI	0.311	0.334
Water (%)	50.0	Zeta potential (mV)	-22.736	-21.50

3.4 Testing of kinetic stability of nanoemulsions

Nanoemulsions represent a kinetically stable colloidal arrangement, formulated with precise ratios of oil, surfactant, and water, and are distinguished by the lack of separation of phase, creaming, and cracking. (Sharma et al., 2012) [44]. The optimized nanoemulsion, developed using a 3-factor, 3-level design of Box–Behnken coupled with (RSM) response surface methodology, was put through to distress assessments of stability, including cycles of heating–cooling, centrifugation, and cycles of freeze–thaw. The optimized formulation successfully withstood all stress responses, showing no evidence of Ostwald ripening, thereby confirming its stability.

4. Evaluation of Nanoemulsion Formulations

4.1 Determination of Globular diameter and Poly Dispersity Index

The globule (diameter) size and distribution of the optimized nanoemulsion are presented in (Fig. 4). The formulation exhibited an average globule size of 118.3 ± 7 nm with a low polydispersity index (0.387 ± 0.023), indicating uniformity in particle distribution.

Further characterization using transmission electron microscopy (TEM) provided detailed insights into the morphology and droplet distribution of the dispersed phase. TEM images revealed that the droplets in the optimized formulation were predominantly spherical with sizes ranging between 22.10 and 94.80 nm (Fig. 4).

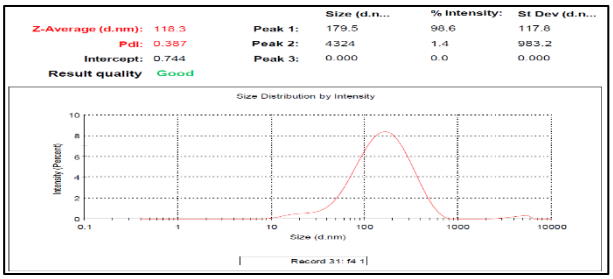

Fig. 4. Particle/ size of globule and Polydispersity index (PDI) of optimized nano-emulsion formulation

4.2 Electrokinetic (Zeta) Potential Determination

The zeta potential of the optimized RXN nanoemulsion was computed at –21.73 ± 5.67 mV (Fig. 5). Previous studies have reported that oil droplets stabilized by non-ionic surfactants exhibit characteristic surface charges, reflected in their (electrokinetic) zeta potential values. The negative zeta potential observed in this formulation indicates the presence of a net negative charge on the droplet surface, which contributes to force of repulsive electrostatic and, thereby enhances the stability of the system. Across the experimental runs, zeta potential values ranged from –14.56 mV to –29.54 mV, confirming consistency within the stability range.

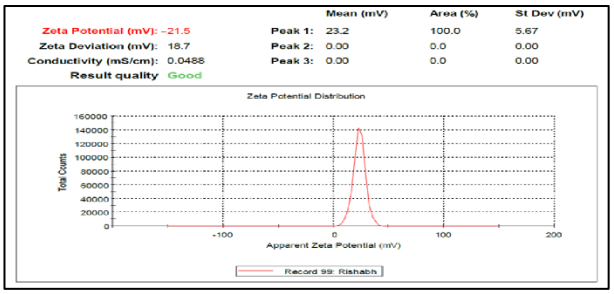

Fig. 5. zeta potential of optimized nano-emulsion formulation

4.3 Determination of Structure of Surface by TEM Analysis

The structure of surface analysis was executed by Transmission electron microscopy (TEM) to gain deeper insights into the nature of surface and spatial arrangement of particles within the nanoemulsion system. In the optimized NEG formulation, the majority of particles exhibited a uniform, spherical shape with sizes ranging from 22.10–180.10 nm (Fig. 6). The particle size distribution observed through TEM was consistent with the statistical range obtained from photon correlation spectroscopy, thereby confirming good agreement between both characterization techniques.

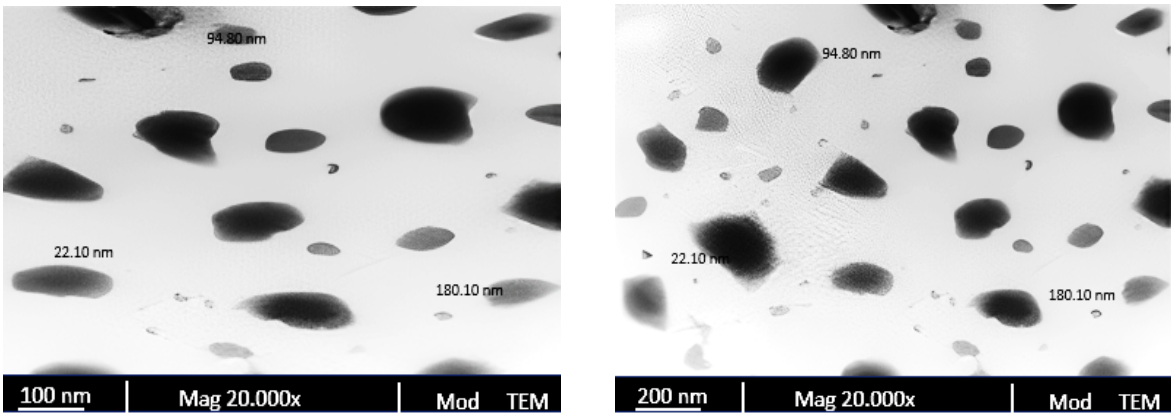

Fig. 6. Surface Morphology/ TEM Analysis of optimized Nanoemulgel

4.4 Preparation of RXN Nanoemulsion Gel/ Nanoemulgel (NEG)

Optimized nanoemulsion containing 100 mg of RXN was incorporated dropwise into the gel base sol system under steady stirring to achieve uniform mixing, subsequently stored at 4°C for 24 hours. The resulting gel was assessed for critical criteria, including zeta potential, polydispersity index (PDI), and size of vesicle of the optimized RXN nanoemulgel. Initially, the optimized RXN nanoemulsion exhibited relatively low viscosity; however, upon conversion into RXN nanoemulgel, the formulation displayed enhanced viscosity, making it more suitable for prolonged site-specific application. Carbopol 934P, used as the gelling agent, facilitated the transformation of RXN nanoemulsion into RXN nanoemulgel, thereby improving drug permeability through gingival tissue. The final optimized RXN nanoemulsion Carbopol gel demonstrated a smooth texture, uniform consistency, and an aesthetically acceptable appearance.

5. Evaluation of Roxithromycin loaded nanoemulgel

5.1 Determination of pH of Nanoemulgel

The pH of the optimized nanoemulgel (NEG-9) has been assessed to determine its compatibility with the physiological pH levels of saliva and SGCF, which range from 5.5 to 8.0. For this evaluation, 0.5 g of the formulation had been dissolved in distilled water (50mL) and subsequently stored at 4°C. The pH was obtained with a digital pH meter at the initial time point and subsequently at intervals over a period of 21 days. Measurements have been taken in triplicate, and their average readings were reported.

Table 5. pH determination at different temperatures of Optimized Nanoemulgel (NEG-9)

S.No.	Time (in days)	pH at different Temperature		
		8ºC	25ºC	37ºC
1	0	6.71±0.021	6.83 ± 0.006	6.74 ± 0.004
2	7	6.67 ± 0.023	6.64 ± 0.011	6.66 ± 0.054
3	14	6.66 ± 0.021	6.56 ± 0.002	6.67 ± 0.023
4	21	6.56 ± 0.004	6.63 ± 0.018	6.66 ± 0.021

Day 0*: indicates freshly prepared formulation

5.2 Measurement of Sol-gel transition

The temperature of gelation was observed within the range of 22.00 ± 0.36°C to 25.21 ± 0.41°C, while the gelling time varied between 35.43 ± 0.63 and 37.22 ± 0.66 seconds.

5.3 Syringeability

The ease of syringeability was assessed qualitatively. The ease of syringeability was observed visually. The optimized formulation NEG-9 had passed the Syringeability test.

5.4 Homogeneity test

The optimized RXN nanoemulsion gel demonstrated a smoothness in texture with a homogeneous and aesthetically acceptable in manner. No gritty particles were spotted, and the formulation showed no indication of phase separation when compared with the standards. (Varshosaz et al., 2002) [47].

5.5 Spreadability Study

Spreadability is a critical characteristic of gels, reflecting easily implementable and formulation consistency. The optimized RXN nanoemulgel (NEG-9) demonstrated excellent spreadability, with spreading diameters of 5.83 ± 0.06 cm on day 0 and 5.00 ± 0.01 cm on day 9. No significant change in spreading diameter was observed over the 9-day period, indicating stable spreadability of the formulation.

5.6 Extrudability test

The extrudability of the optimized RXN nanoemulgel (NEG-9) was evaluated and found to be satisfactory, indicating smooth extrusion from the collapsible tube under moderate pressure. The formulation demonstrated consistent extrusion without any signs of phase separation or blockage. Quantitatively, the extrudability of NEG-9 was measured as 1.97±0.12 g on day 0 and 1.75±0.12 g on day 9. No remarkable difference was noticed over the study period, confirming the stability and suitability of the formulation for practical application.

5.7 Thermal Analysis of the RXN Nanoemulgel

The peak shown in Fig. 7 suggests that roxithromycin experiences a phase transition at about 123.65ºC, which aligns closely with the previously reported temperature of 125ºC (Al Hossain et al., 2019) [48]. The analysis of thermal highlighted a evident peak with endothermic characteristics, supporting the crystalline nature of the drug. In contrast, the DSC thermal analysis of the optimized RXN nanoemulgel, depicted in Fig. 8, did not show a distinct peak related to the drug. This absence of a sharp peak indicates that there is no drug leakage from the formulation.

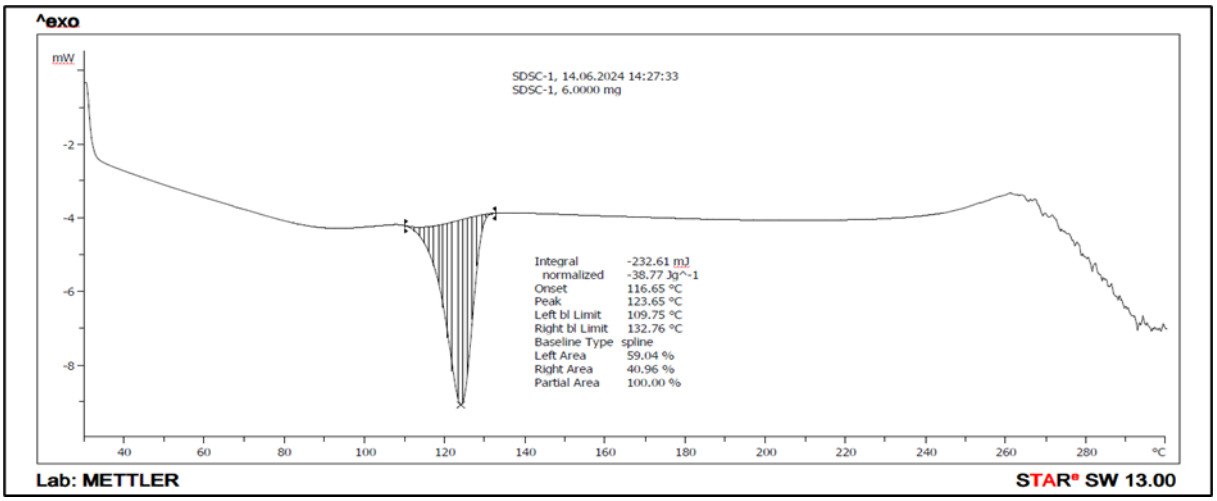

Fig. 7. Thermoanalysis graph of drug Roxithromycin

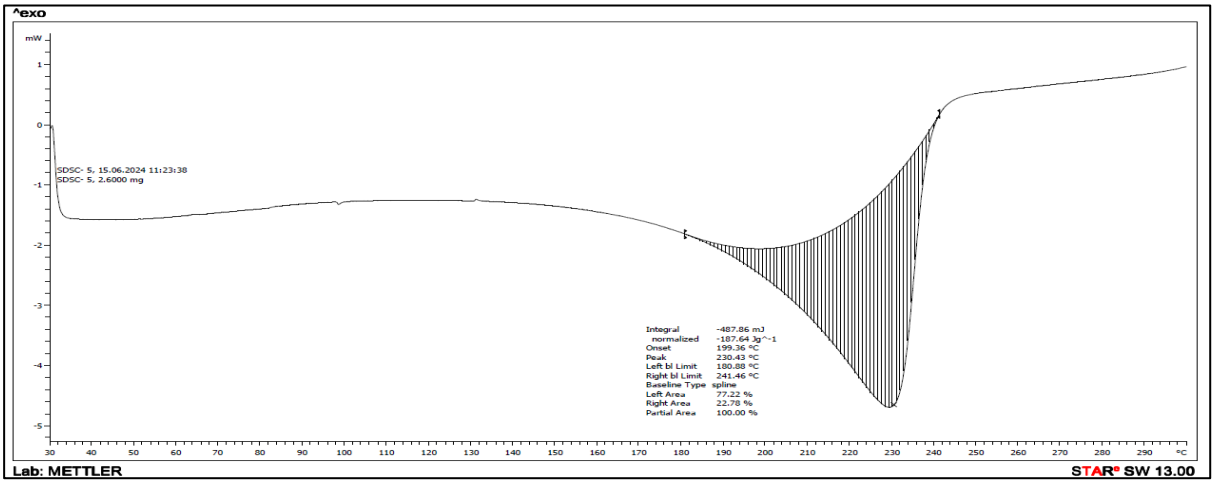

Fig. 8. Thermoanalysis graph of optimized RXN Nanoemulgel

5.8 Measurement of Rheology of Nanoemulgel

Viscosity is a crucial factor for drug infiltrated and is linked to the viscosity of the nanoemulgel. The viscosity of the formulated nanoemulgel remained constant, making it ideal for application on thin layers of skin or gingival tissues. (Srivastava et al., 2016b) [49]. The aspect of flow the RXN loaded NEG at temperatures of 4± 2ºC, 25±2ºC, and 37±2ºC were illustrated in Figures 9, 10, 11, and 12. In steady shear rheological observation, the optimized RXN NEG displayed a viscoelastic (non-Newtonian) and non-linear relationship between force of shear and rate of shear, exhibiting pseudoplastic behavior typical of hydrophilic polymeric systems. This characteristic is significant as it enhances spreading when applied to biological surfaces. Generally, aqueous affinity polymeric systems show non-Newtonian, shear thinning (pseudoplastic), which aids in their spreadability upon application; a greater degree of pseudoplasticity enhances the formulation's ease of spreading (Rhee et al., 2008) [50]. The rheological study results indicate that the optimized gel in sol form at 4±2ºC transitions to gel at 25±2ºC and becomes firmer at 37±2ºC, confirming its appropriate sol-gel properties for locally inserted periodontal drug delivery, with all findings summarized in tables 6, 7, and 8. Ultimately, by fitting the studied rheological aspects to various standards using software Rheo 3000 (Brookfield Engineering Laboratories, Inc.), the Herschel–Bulkley model was identified as the most suitable to describe the flow aspect of the optimized formulation. The flow characteristics are crucial for facilitating the administration of the product into the periodontal pocket.

Table 6. Viscosity at 25°C of Optimized Nanoemulgel (NEG-9)

Spindle	RPM (Shear Rate)	Viscosity (cP)	Temperature (°C)	Observation
LV-4	10	2,400	25	Thick and spreadable
LV-4	20	1,850	25	Starts to thin
LV-4	50	1,200	25	Easily flowable, good injectability

Table 7. Viscosity at 37°C of Optimized Nanoemulgel (NEG-9)

Spindle	RPM (Shear Rate)	Viscosity (cP)	Temperature (°C)	Observation
LV-4	10	2100	37	High viscosity, stable gel
LV-4	20	1600	37	Shear-thinning begins
LV-4	50	1100	37	Easily spreadable

Table 8. Viscosity at 4°C of Optimized Nanoemulgel (NEG-9)

Spindle	RPM (Shear Rate)	Viscosity (cP)	Temperature (°C)	Observation
LV-4	10	2700	4	Slightly thicker than at 37°C (Gel stiffness)
LV-4	20	2100	4	Gel retains structure
LV-4	50	1700	4	Shear-thinning confirmed

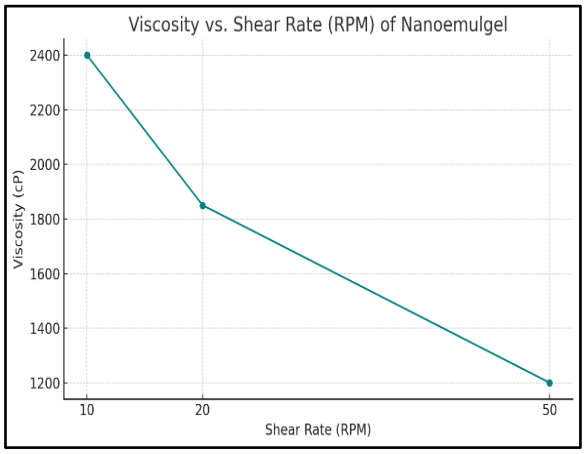

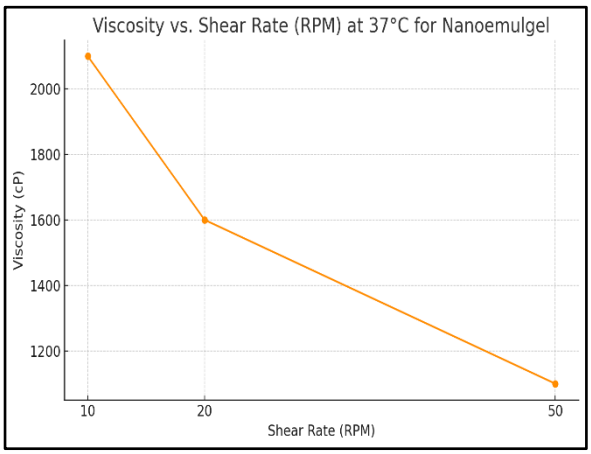

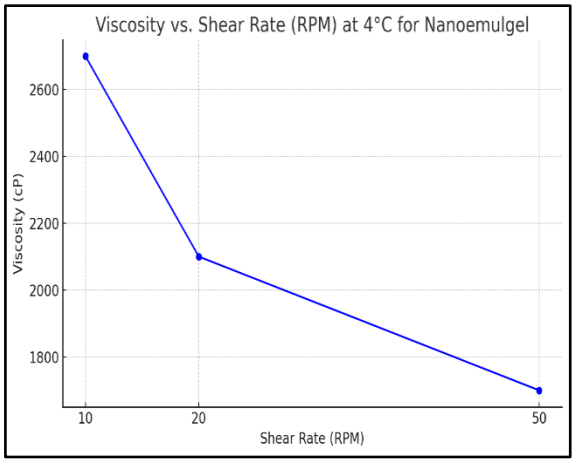

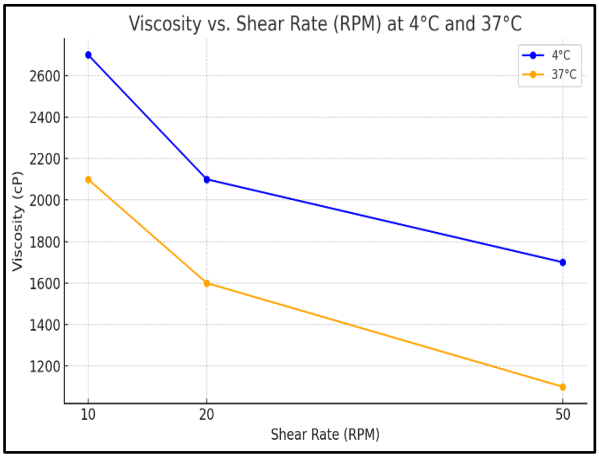

Fig. 9. Graphical Plot of viscosity at 25ºC, 37ºC & 4ºC between viscosity and shear rate, Comparative Graphical Plot of viscosity vs shear rate for the nanoemulgel at 4°C and 37°C

5.8 Drug content Determination

The RXN infused NEG formulations presented in this study exhibited varying contents of the polymer Carbopol 934P, resulting in formulations with a broad spectrum of consistency. (Dabbir et al., 2013) [51]. The drug content of the optimized RXN nanoemulgel (NEG-3), (NEG-5) and (NEG-9) were determined to assess uniformity and accuracy of drug incorporation. In the observation, the drug content of optimized formulations (NEG-3), (NEG-5) and (NEG-9) were nearly same and in ranged between 97.81±0.83%, 98.53±0.11% and 100.12±0.55% (Table 9). The outcome stipulated that addition of medicament in NEGs adjudged insignificant loss of the medicament. The formulation exhibited high drug content with values close to the theoretical amount, indicating efficient entrapment of roxithromycin within the gel matrix. The results confirmed uniform distribution of the drug throughout the formulation, ensuring suitability for local drug delivery applications. (Zheng et al., 2016) [52].

Table 9. % Durg Content of Optimized Nanoemulgel (NEG-9), (NEG-5) and (NEG-9)

S.No.	Optimized Formulation	% Drug Content
1	NEG-3	97.81±0.83
2	NEG-5	98.53±0.11
3	NEG-9	100.12±0.55

5.9 in-vitro release testing and kinetics of release of NEG with RXN

Profile of drug as in-vitro release was executed in SGCF (phosphate buffer, pH 6.8) utilizing the diffusion method. The pattern of release for the optimized formulation, as shown in Fig. 13, exhibited an initial spurt release of the drug, succeeded by extended-release phase. (Patel et al., 2024) [53]. The early swift release can be linked to the existence of nanodroplets situated at the superficial of the NEG. Following a 24-hour period, the total drug release achieved was 77.69%, which supports the observed sustained release characteristics. The results demonstrate that the NEG formulation successfully promoted a properly controlled and prolonged release of RXN.

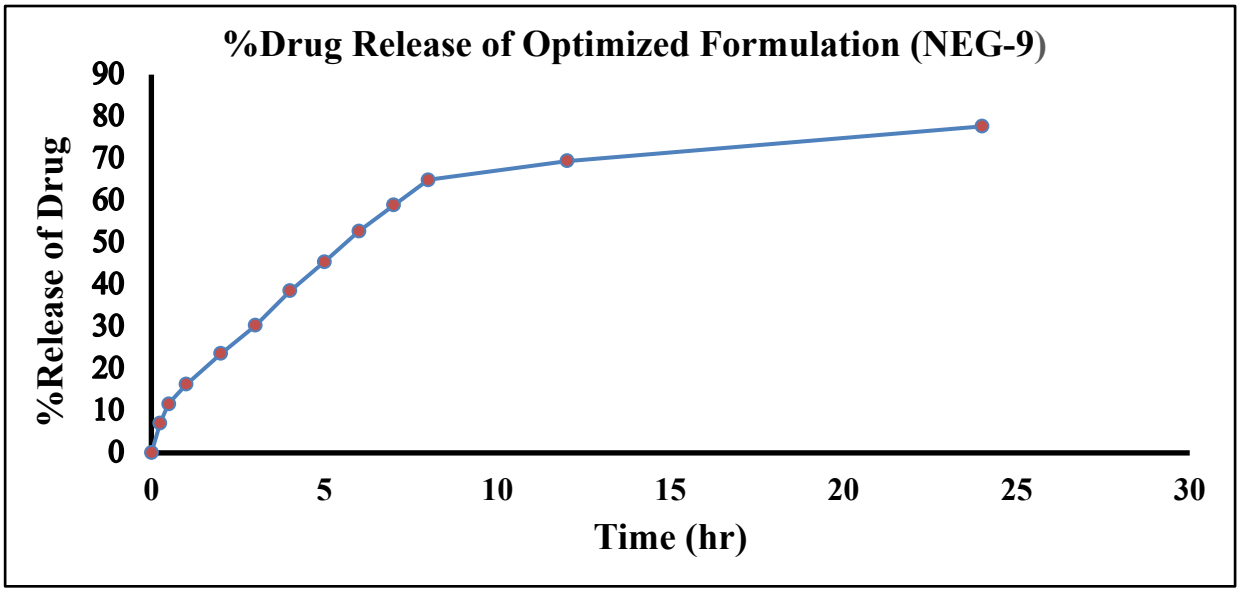

Fig. 10. Graphical Representation of profile of % drug release study of optimized Nanoemulgel (NEG-9)

5.10 study of *Ex-vivo* Tissue Permeation

This method has been employed to evaluate the permeability of the nanoemulgel, focusing on its potential to achieve targeted and localized drug delivery by retaining the drug within the tissue and minimizing systemic absorption. Such localization helps to mitigate systemic adverse reaction and lowers the likelihood of resistance of antimicrobial Less than 50% of the medication infiltrated the buccal mucosa, according to the findings, while the majority remained entrapped within the tissue. This retention suggests that the system accouters a localized therapeutic response, with the medication being incorporated into the bilayer phospholipid of the buccal region. (Angellotti et al., 2021) [54].

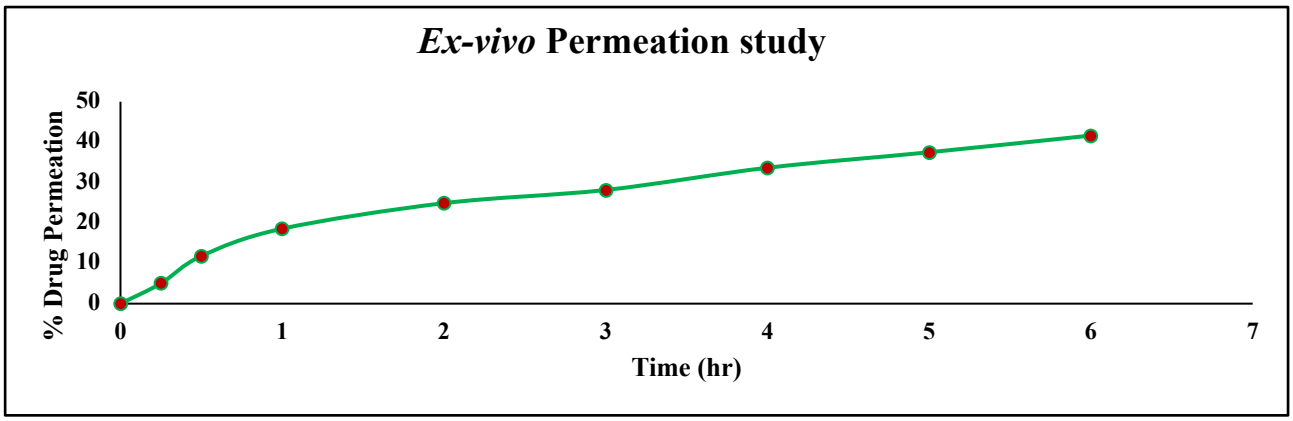

Fig. 11. *Ex-vivo* permeation of roxithromycin from buccal mucosa of goat

5.10 Strength of *Ex-vivo* mucoadhesive

The maximum observed force of mucoadhesion of the nanoemulgel formulations (NEGs) was found to be 32.69±0.91 g, which indicates stronger adhesion between formulation and mucosal tissue. This level of mucoadhesive strength is sufficient to ensure extended residence duration and localized drug retention at the zone of application, while remaining within a safe range that does not cause mucosal irritation or discomfort. These findings confirm the suitability of the formulation for local drug delivery approaches.

5.11 Antibacterial Activity

The optimized nanoemulgel containing ROX and eugenol as the oil phase (NEG-9) demonstrated a more pronounced antibacterial effect against *E. coli* and *S. aureus*, exhibiting growth zones of inhibition of 24.1±0.34 mm and 18.7±0.36 mm, respectively. In comparison, eugenol gels alone resulted in growth zones

of inhibition of 11.5±0.24 mm for *S. aureus* and 9.2±0.22 mm for *E. coli*. The stronger antibacterial activity of the NEG which includes eugenol, in contrast with eugenol alone, is due to the presence of eugenol in nano-droplet form within the NEG. This facilitates a more efficient merger with the outer membrane of microbes, while the surfactants in the NEG can hinder the external membrane, triggering microbial death. (Awadh et al., 2025) [55].

Table 10. Antibacterial study of Placebo Nanoemulgel and Optimized Formulation (NEG-9) on *Stephylococcus aureus*

Time (in hr)	Zone of inhibition (mm) *Stephylococcus aureus*	
	Placebo gel (Eugenol as oil phase without drug)	Optimized ROX loaded Nanoemulgel (NEG-9)
0	0	0
0.5	2.4±0.05	8.9±0.12
1	3.6±0.09	11.7±016
2	5.4±0.12	14.2±0.20
4	7.2±0.16	18.5±0.24
8	9.4±0.19	20.8±0.29
12	10.1±0.21	22.6±0.32
24	11.5±0.24	24.1±0.34

Table 11. Antibacterial study of Placebo Nanoemulgel and Optimized Formulation (NEG-9) on *Escherichia coli*

Time (in hr)	Zone of inhibition (mm) *Escherichia coli*	
	Placebo gel (Eugenol as oil phase without drug)	Optimized ROX loaded Nanoemulgel (NEG-9)
0	0	0
0.5	0.6±0.01	4.7±0.09
1	1.3±0.04	6.6±0.12
2	2.6±0.06	9.0±0.17
4	3.9±0.10	11.5±0.18
8	5.7±0.14	13.6±0.26
12	7.6±0.16	16.2±0.29
24	9.2±0.22	18.7±0.36

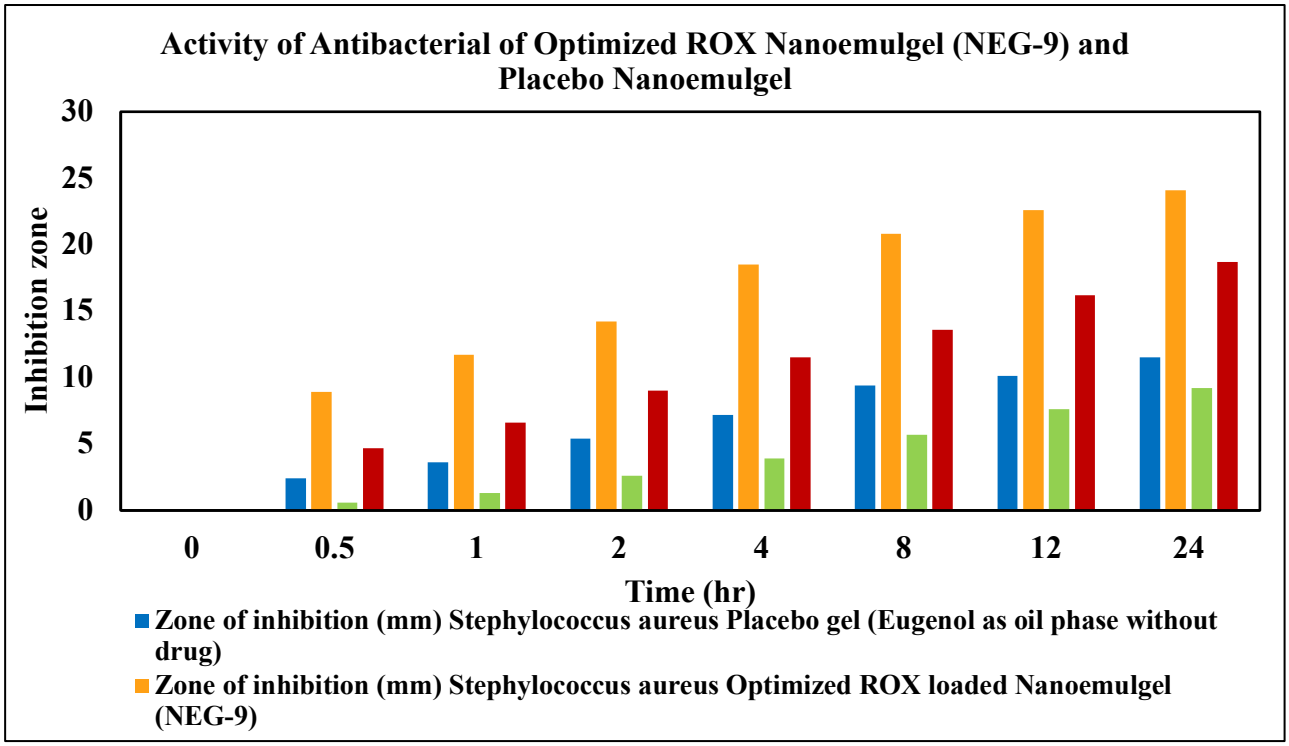

Fig. 12. Graphical representation of Antibacterial study of Optimized ROX Nanoemulgel (NEG-9) and Placebo Nanoemulgel

5.12 Stability Studies of Optimized Nanoemulgel

The stability of the optimized nanoemulgel formulation has been assessed through evaluations of pH, homogeneity, and color. No significant variations in organoleptic properties were detected, and the formulation remained homogeneous for up to three months at 25°C. Similarly, at 5°C and 40°C, no noticeable change in color was observed. The pH of the formulation also remained unaffected under different storage conditions. At 5°C, the formulation preserved its homogeneity, although slight variations in spreadability and viscosity were noted. The nanoemulgel exhibited kinetic stability and remained stable at 40°C; however, under this condition, spreadability increased, viscosity decreased, and a progressive color change from white to off-white was observed. (Das et al., 2020) [56].

Table 12. Study of stability of Optimized nanoemulgel at 25°C

Days	Uniformity Nature	pH	Spreadability (cm)	Viscosity (cP)	Centrifugation	Color
1	Homogeneous	6.8±0.1	5.81±0.06	2600±5	Stable	White
7	Homogeneous	6.8±0.1	5.77±0.04	2612±8	Stable	White
14	Homogeneous	6.8±0.1	5.53±0.02	2623±9	Stable	White
21	Homogeneous	6.7±0.1	5.51±0.01	2645±10	Stable	White
30	Homogeneous	6.6±0.1	5.52±0.01	2657±8	Stable	White
45	Homogeneous	6.8±0.1	5.51±0.01	2671±5	Stable	White
60	Homogeneous	6.7±0.1	5.31±0.01	2683±6	Stable	White
90	Homogeneous	6.5±0.1	5.01±0.01	2696±8	Stable	White

Table 13. Study of stability of Optimized nanoemulgel at 5°C

Days	Uniformity Nature	pH	Spreadability (cm)	Viscosity (cP)	Centrifugation	Color
1	Homogeneous	6.8±0.1	5.56±0.06	2755±5	Stable	White
7	Homogeneous	6.8±0.1	5.52±0.04	2779±6	Stable	White

14	Homogeneous	6.7±0.1	5.51±0.02	2822±9	Stable	White
21	Homogeneous	6.7±0.1	5.51±0.01	2933±8	Stable	White
30	Homogeneous	6.7±0.1	5.3±0.01	3014±8	Stable	White
45	Homogeneous	6.8±0.1	5.21±0.01	3235±5	Stable	White
60	Homogeneous	6.7±0.1	5.11±0.01	3456±6	Stable	White
90	Homogeneous	6.6±0.1	4.89±0.01	3780±8	Stable	White

Table 14. Study of stability of Optimized nanoemulgel at 40°C

Days	Uniformity Nature	pH	Spreadability (cm)	Viscosity (cP)	Centrifugation	Colour
1	Homogeneous	6.8±0.1	5.04±0.06	2758±4	Stable	White
7	Homogeneous	6.8±0.1	5.09±0.04	2704±8	Stable	White
14	Homogeneous	6.7±0.1	5.53±0.02	2621±9	Stable	White
21	Homogeneous	6.7±0.1	5.61±0.01	2544±8	Stable	White
30	Homogeneous	6.7±0.1	5.70±0.01	2386±7	Stable	White
45	Homogeneous	6.7±0.1	5.77±0.01	2337±7	Stable	White
60	Heterogeneous	6.6±0.1	5.9±0.01	2268±6	Unstable	Off-White
90	Heterogeneous	6.6±0.1	6.1±0.01	2015±6	Unstable	Off-White

Viscosity enacts a pivotal role in pharmaceutical forms, as it directly influences drug release and the coherence of dosage form as semisolid (Gupta et al., 2019) [57]. In the present study, a decrease in viscosity of the nanoemulgel was observed with increasing temperature from 5°C to 40°C. Correspondingly, spreadability increased as viscosity decreased, reflecting the inverse relationship between these two parameters. Similar trends in semisolid formulations have also been reported. Based on these observations, room temperature (25°C) was revered appropriate storage condition for the nanoemulgel. The enhanced spreadability at higher temperatures may offer clinical advantages, particularly for buccal applications where the local temperature exceeds room temperature, thereby facilitating administration. In terms of physical stability, the formulation remained stable for up to three months, with no evidence of phase separation following centrifugation at 3000 rpm for 15 minutes (Tables 12–14).

6.0 Conclusion

The roxithromycin-loaded nanoemulgel was developed using eugenol as the oil phase and optimized through a design of experiments approach. Phase diagrams constructed at distinct S_{mix} ratios indicated that the 6:1 S_{mix} ratio exhibited the widest region of nanoemulsion. A spontaneous emulsification technique was employed to formulate fine nanoemulsion, which were subsequently incorporated into Carbopol 934P gel base to obtain the final nanoemulgel formulation. Transmission electron microscopy (TEM) confirmed the uniform globular size and smooth surface of the dispersed nanodroplets. Evaluation of the roxithromycin nanoemulgel demonstrated its suitability for the management of periodontal disease, showing enhanced therapeutic efficacy with reduced side effects by facilitating localized drug delivery into the periodontal pocket.

REFERENCE

1. Tonetti, M. S., Greenwell, H., and Kornman, K. S. (2018). Staging and grading of periodontitis: framework and proposal of a new classification and case definition. J. Clin. Periodontology 45, S159-S172–S161. doi:10.1002/jper.18-0006
2. Sanz, M., Papapanou, P. N., Tonetti, M. S., Greenwell, H., and Kornman, K. (2020). Guest editorial: clarifications on the use of the new classification of periodontitis. J. Clin. Periodontology 47, 658–659. doi:10.1111/jcpe.13286
3. Deo, P. N., and Deshmukh, R. (2019) 'Oral microbiome: Unveiling the fundamentals,' Journal of Oral and Maxillofacial Pathology, 23(1), p. 122. https://doi.org/10.4103/jomfp.jomfp_304_18.
4. Santosh, A.B.R.; Muddana, K.; Bakki, S.R. (2021). Fungal infections of oral cavity: Diagnosis, management, and association with COVID-19. SN Compr. Clin. Med. 3, 1373–1384.
5. Gandhi, U.H. et al. (2025). The effectiveness of metronidazole as a localized drug delivery system in the treatment of periodontal diseases: a narrative

review,' Cureus [Preprint]. https://doi.org/10.7759/cureus.80547.

6. Jonesn, G.; Wilson, H.; Smith, S.; Brown, T. (2023) Periodontitis: Causes, symptoms, and steps to treatment. Fusion Multidiscip. Res. 4, 445–457.

7. Yin, Y.; Yang, S.; Ai, D.; Qin, H.; Sun, Y.; Xia, X.; Xu, X.; Ji, W.; Song, J. (2023) 'Rational Design of Bioactive Hydrogels toward Periodontal Delivery: From Pathophysiology to Therapeutic Applications,' Advanced Functional Materials, 33(30). https://doi.org/10.1002/adfm.202301062.

8. Maurya R, Singh MP and Kymonil KM, (2019). Formulation and evaluation of moxifloxacin microspheres implant for intra-periodontal pockets. Int J Pharm Sci & Res 10(8): 3891-97. doi: 10.13040/IJPSR.0975-8232.10(8). 3891-3897

9. Maurya R, Kumar P, Tiwari G. (2024) Rationalization Progress of Novel Drug Delivery System for Intra-Periodontal Pockets Against Periodontitis. Pharm Nanotechnol. doi: 10.2174/0122117385334802241122094148

10. Sanz. M, Herrera. D, and Kebschull. M, (2020). Treatment of stage I–III periodontitis—The EFP S3 level clinical practice guideline. Journal of Clinical Periodontology, 47(S22), pp. 4–60. https://doi.org/10.1111/jcpe.13290.

11. Ilyes, I., Boariu, M., Rusu, D., Iorio-Siciliano, V., Vela, O., Boia, S., Radulescu, V., Șurlin, P., Jentsch, H., Lodin, A., & Stratul, S.-I. (2024). Comparative Study of Systemic vs. Local Antibiotics with Subgingival Instrumentation in Stage III–IV Periodontitis: A Retrospective Analysis. Antibiotics, 13 (5), pp 1-16. https://doi.org/10.3390/antibiotics13050430

12. Slots J, Ting M: (2002). Systemic antibiotics in the treatment of periodontal disease . Periodontol 2000., 28:106-76. 10.1034/j.1600-0757.2002.280106.x

13. Mehravani M, Houshyar E, Jamalnia S, Gharaaghaji R, (2024) Effects of local and systemic metronidazole as adjunctive treatment in chronic periodontitis patients. Clin Exp Dent Res. 10:e70050. 10.1002/cre2.70050

14. Kapoor A, Malhotra R, Grover V, Grover D, (2012). Systemic antibiotic therapy in periodontics. Dent Res J (Isfahan)., 9:505-15. 10.4103/1735-3327.104866

15. Loesche WJ, (1996). Antimicrobials in dentistry: with knowledge comes responsibility. J Dent Res. 75:1432-3. 10.1177/00220345960750070101

16. Orive, G., Hernandez, R.M., Rodriguez Gascon, A., Dominguez-Gil, A., Pedraz, J.L., (2003). Drug delivery in biotechnology: present and future. Curr. Opin. Biotechnol. 14, 659–664. https://doi.org/10.1016/j.copbio.2003.10.007.

17. Koopaei MN, Maghazei MS, Mostafavi SH, Jamalifar H, Samadi N, Amini M, Malek SJ, Darvishi B, Atyabi F, Dinarvand R. (2012). Enhanced antibacterial activity of roxithromycin loaded pegylated poly lactide-co-glycolide nanoparticles. Daru. 20 (1):92. doi: 10.1186/2008-2231-20-92. PMID: 23351784; PMCID: PMC3607925.

18. Srivastava, M., Neupane, Y.R., Kumar, P., Kohli, K., (2016b). Nanoemulgel (NEG) of Ketoprofen with eugenol as oil phase for the treatment of ligature-induced experimental periodontitis in Wistar rats. Drug Deliv. 23 (7), 2228–2234. 10.3109/10717544.2014.958625.

19. Ahmad, N., Ahmad, R., Alam, M.A., Ahmad, F.J., (2018a). Quantification and brain targeting of eugenol-loaded surface modified nanoparticles through intranasal route in the treatment of cerebral ischemia. Drug Res. (Stuttg). https://doi.org/10.1055/a-0596-7288.

20. Hong, C.H., Hur, S.K., Oh, O.J., Kim, S.S., Nam, K.A., Lee, S.K., (2002). Evaluation of natural products on inhibition of inducible cyclooxygenase (COX-2) and nitric oxide synthase (iNOS) in cultured mouse macrophage cells. J. Ethnopharmacol. 83 (1–2), 153–159. 10.1081/ddc-120028715.

21. Jadhav BK, Khandelwal KR, Ketkar AR, Pisal SS. Formulation and evaluation of mucoadhesive tablets containing eugenol for the treatment of periodontal diseases. Drug Dev Ind Pharm. 2004 Feb;30(2):195-203. doi: 10.1081/ddc-120028715.

22. Shakeel, F., Ramadan, W., Faisal, M.S., Rizwan, M., Faiyazuddin, M., Mustafa, G., Shafiq, S., 2010. Transdermal and topical delivery of anti-inflammatory agents using nanoemulsion/microemulsion: an updated review. Curr. Nanosci. 6, 184–198.

23. Srivastava, M., Kohli, K., & Ali, M. (2014). Formulation development of novel in situ nanoemulgel (NEG) of ketoprofen for the treatment of periodontitis. Drug Delivery, 23(1), 154–166. https://doi.org/10.3109/10717544.2014.907842

24. Nasra MM, Khiri HM, Hazzah HA, Abdallah OY. (2017) Formulation, in-vitro characterization and clinical evaluation of curcumin in-situ gel for treatment of periodontitis. Drug Deliv. 24(1):133-142. doi: 10.1080/10717544.2016.1233591.

25. Jones DS, Bruschi ML, de Freitas O, Gremião MP, Lara EH, Andrews GP. (2009). Rheological, mechanical and mucoadhesive properties of thermoresponsive, bioadhesive binary mixtures composed of poloxamer 407 and carbopol 974P

designed as platforms for implantable drug delivery systems for use in the oral cavity. Int J Pharm. 8372(1-2):49-58. doi: 10.1016/j.ijpharm.2009.01.006. Epub 2009. PMID: 19429268.

26. Garala K, Joshi P, Shah M, Ramkishan A, Patel J. (2013). Formulation and evaluation of periodontal in situ gel. Int J Pharm Investig. 3(1):29-41. doi: 10.4103/2230-973X.108961.

27. Govender S, Pillay V, Chetty DJ, et al. (2005). Optimisation and characterisation of bioadhesive controlled release tetracycline microspheres. Int J Pharm 306:24–40.

28. Shafiq S, Shakeel F, Talegaonkar S, et al. (2007). Formulation development and optimization using nanoemulsion technique: a technical note. AAPS PharmSciTech 8(2): E12–E17.

29. Bali V, Ali M, Ali J. (2010). Study of surfactant combinations and development of a novel nanoemulsion for minimising variations in bioavailability of ezetimibe. Coll Surf B Biointerface 76:410–20.

30. N. Belhaj, F. Dupuis, E. Arab-Tehrany, F. M. Denis, C. Paris, I. Lartaud, and M. Linder (2012). Formulation, characterization and pharmacokinetic studies of coenzyme Q10 PUFA's nanoemulsions. Eur. J. Pharm. Sci. 47, 305–312.

31. M. Srivastava, K. Kohli, and M. Ali (2016). Formulation development of novel in situ nanoemulgel (NEG) of ketoprofen for the treatment of periodontitis. Drug Deliv. 23(1), 154–166. https://doi.org/10.3109/10717544.2014.907842.

32. Hosny, K.M., Banjar, Z.M., (2013). The formulation of a nasal nanoemulsion zaleplon in situ gel for the treatment of insomnia. Expert Opin. Drug Deliv. 10 (8), 1033–1041.

33. Mahmood A, Mahmood A, Ibrahim MA, Hussain Z, Ashraf MU, Salem-Bekhit MM, Elbagory I. (2023). Development and Evaluation of Sodium Alginate/Carbopol 934P-Co-Poly (Methacrylate) Hydrogels for Localized Drug Delivery. Polymers (Basel). 15(2):311. doi: 10.3390/polym15020311. PMID: 36679191; PMCID: PMC9864554.

34. Ahad, A., Al-Saleh, A.A., Al-Mohizea, A.M., Al-Jenoobi, F.I., Raish, M., Yassin, A.E.B., Alam, M.A., (2017). Pharmacodynamic study of eprosartan mesylate-loaded transfersomes Carbopol_ gel under Dermaroller_ on rats with methyl prednisolone acetate-induced hypertension. Biomed. Pharmacother. 89, 177–184.

35. Al-Suwayeh, S.A., Taha, E.I., Al-Qahtani, F.M., Ahmed, M.O., Badran, M.M., (2014). Evaluation of skin permeation and analgesic activity effects of Carbopol lornoxicam topical gels containing penetration enhancer. Sci. World J. 2014,127495.

36. Kumari N, Pathak K. (2012). Dual controlled release, in situ gelling periodontal sol of metronidazole benzoate and serratiopeptidase: statistical optimization and mechanistic evaluation. Curr Drug Deliv 9:74–84.

37. Satpute, S. B., & Balap, A. R. (2024). Evaluation of Wound Healing Activity of Polyherbal Gel Containing Azadirachta indica, A. Juss. and Tridax procumbens L. Extracts. Pharmacognosy Research, 16(4), 968–976.

38. Kandale, J., Sangshetti, J., Dama, G., Bidkar, J., Umbare, R., & Ghangale, G. (2023). Formulation and evaluation of polyherbal emulgel. International Journal of Experimental Research and Review, 30, 296–305.

39. Shaikh AR, Giridhar R, Megraud F, Yadav MR. (2009). Metalloantibiotics: synthesis, characterization and antimicrobial evaluation of bismuth-fluoroquinolone complexes against Helicobacter pylori. Acta Pharm. 59, 259–71. doi: https://doi.org/10.2478/v10007-009-0027-6

40. Cordeiro KC, Scaffo J, Flexa BN, Gama CCA, Ferreira MA, Cruz RAS, (2023). Characterization of bergamot essential oil: chemical, microbiological and colloidal aspects. Braz J Biol. 15, 1–6. doi: https://doi.org/10.1590/1519-6984.275622.27

41. Hafez HN, Alshammari AG, El-Gazzar AR. (2015). Facile heterocyclic synthesis and antimicrobial activity of polysubstituted and condensed pyrazolopyranopyrimidine and pyrazolopyranotriazine derivatives. Acta Pharm. 65, 399–412. doi: https://doi.org/10.1515/acph- 2015-0037

42. Bruschi ML, Jones DS, Panzeri H, et al. (2007). Semisolid systems containing propolis for the treatment of periodontal disease: in vitro release kinetics, syringeability, rheological, textural, and mucoadhesive properties. J Pharm Sci 96, 2074–89.

43. Sharma S, Kumar A, Sahni JK, et al. (2012). Nanoemulsion based hydrogel containing omega 3 fatty acids as a surrogate of betamethasone dipropionate for topical delivery. Adv Sci Lett 6: 221–31.

44. Sohail, M.; Naveed, A.; Abdul, R.; Khan, H.M.; Khan, H. (2018). An approach to enhanced stability: Formulation and characterization of Solanum lycopersicum derived lycopene based topical emulgel. Saudi Pharm. J. 26, 1170–1177. [CrossRef]

45. Ullah N, Amin A, Farid A, Selim S, Rashid SA, Aziz MI, Kamran SH, Khan MA, Rahim Khan N, Mashal S, Mohtasheemul Hasan M. (2023). Development and Evaluation of Essential Oil-Based Nanoemulgel Formulation for the Treatment of Oral

Bacterial Infections. Gels. Mar 21;9(3):252. doi: 10.3390/gels9030252. PMID: 36975701; PMCID: PMC10048686.
46. Varshosaz, J., Tavakoli, N., Saidian, S., (2002). Development and physical characterization of a periodontal bioadhesive gel of metronidazole. Drug Deliv. 9 (2), 127–133.
47. Al Hossain, A.S.M.M.; Sil, B.C.; Iliopoulos, F.; Lever, R.; Hadgraft, J.; Lane, M.E. (2019). Preparation, Characterisation, and Topical Delivery of Terbinafine. Pharmaceutics, 11, 548. [CrossRef] [PubMed]
48. Srivastava, M., Neupane, Y.R., Kumar, P., Kohli, K., (2016b). Nanoemulgel (NEG) of Ketoprofen with eugenol as oil phase for the treatment of ligature-induced experimental periodontitis in Wistar rats. Drug Deliv. 23 (7), 2228–2234. 10.3109/10717544.2014.958625.
49. Rhee. Y.S., Chang. S.Y., Park. C.W., (2008). Optimization of ibuprofen gel formulations using experimental design technique for enhanced transdermal penetration. Int J Pharm 364:14–20.
50. M. R. Dabbir., and N. R. Sheth., (2013). Formulation development of physiological environment responsive periodontal drug delivery system for local delivery of metronidazole benzoate. Drug Dev Ind Pharm. 39(3), 425–436. https://doi.org/10.3109/03639045.2012.662505
51. Y. Zheng., W. Q. Ouyang., Y. P. Wei., S. F. Syed., C. S. Hao., B. Z. Wang., and Y. H. Shang., (2016). Effects of Carbopol_934 proportion on nanoemulsion gel for topical and transdermal drug delivery: a skin permeation study. Int. J. Nanomed. 11, 5971–5987.
52. Gupta. A., Eral. H.B., (2019). Phase inversion dynamics and droplet size control in spontaneous emulsification. Chem Eng Sci. 197, 100–10. doi: https://doi.org/10.1016/j.ces.2018.11.034
53. Patel, A., & Patel, R. (2024). Development and characterization of lansoprazole nanosponges for enhanced solubility and controlled drug release. Research Square. https://doi.org/10.21203/rs.3.rs-4826853/v1
54. Angellotti G, Presentato A, Murgia D, Di Prima G, D'Agostino F, Scarpaci AG, D'Oca MC, Alduina R, Campisi G, De Caro V. (2021). Lipid Nanocarriers-Loaded Nanocomposite as a Suitable Platform to Release Antibacterial and Antioxidant Agents for Immediate Dental Implant Placement Restorative Treatment. Pharmaceutics. 13(12):2072. doi: 10.3390/pharmaceutics13122072. PMID: 34959353; PMCID: PMC8706998.
55. Ibn Awadh, H., Ahmed, M. (2025). In vitro antibacterial activity of selected plant extracts against Escherichia coli and Staphylococcus aureus bacterial strains. Discov Appl Sci 7, 287. https://doi.org/10.1007/s42452-025-06730-x
56. Das S, Wong ABH. (2020). Stabilization of ferulic acid in topical gel formulation via nanoencapsulation and pH optimization. Sci Rep. 10(1), 12288. doi: 10.1038/s41598-020-68732-6. PMID: 32703966; PMCID: PMC7378829.
57. Sharma. S., Kumar. A., Sahni. .JK., (2012). Nanoemulsion based hydrogel containing omega 3 fatty acids as a surrogate of betamethasone dipropionate for topical delivery. Adv Sci Lett 6: 221–31.